

Universidade Federal de São Carlos  
Centro de Ciências Exatas e de Tecnologia  
Programa de Pós-Graduação em Física

Renan da Silva Souza

# **Effective-Action Approach to Dirty Bosons in Optical Lattices**

São Carlos, Brasil

February, 2019

Universidade Federal de São Carlos  
Centro de Ciências Exatas e de Tecnologia  
Programa de Pós-Graduação em Física

Renan da Silva Souza

# **Effective-Action Approach to Dirty Bosons in Optical Lattices**

Dissertação de Mestrado apresentada ao Programa de Pós-Graduação em Física do Centro de Ciências Exatas e de Tecnologia da Universidade Federal de São Carlos, como um dos requisitos necessários para a obtenção do título de Mestre em Física.

Advisor: Prof. Dr. Francisco Ednilson Alves dos Santos.

São Carlos, Brasil

February, 2019



# UNIVERSIDADE FEDERAL DE SÃO CARLOS

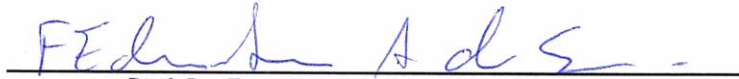
Centro de Ciências Exatas e de Tecnologia  
Programa de Pós-Graduação em Física

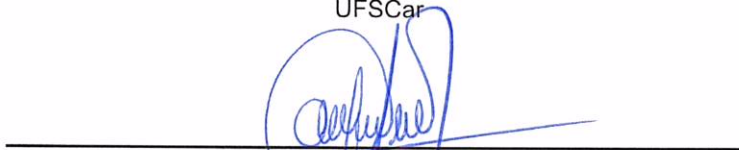
---


## Folha de Aprovação

---

Assinaturas dos membros da comissão examinadora que avaliou e aprovou a Defesa de Dissertação de Mestrado do candidato Renan da Silva Souza, realizada em 21/02/2019:

  
Prof. Dr. Francisco Ednilson Alves dos Santos  
UFSCar

  
Prof. Dr. Celso Jorge Villas Boas  
UFSCar

  
Prof. Dr. Arnaldo Gammal  
IFSC/USP

Certifico que a defesa realizou-se com a participação à distância do(s) membro(s) Arnaldo Gammal e, depois das arguições e deliberações realizadas, o(s) participante(s) à distância está(ao) de acordo com o conteúdo do parecer da banca examinadora redigido neste relatório de defesa.

  
Prof. Dr. Francisco Ednilson Alves dos Santos

# Funding support

This study was financed in part by the Coordenação de Aperfeiçoamento de Pessoal de Nível Superior – Brasil (CAPES) – Finance Code 001.

# Acknowledgements

I would first like to express my deepest gratitude to my advisor Professor Dr. Francisco Ednilson Alves dos Santos of the Physics Department at Universidade Federal de São Carlos. Without his continuous support, motivation and immense knowledge this work would not be completed. I could not have imagined having a better adviser and mentor. Thank you.

My sincere gratitude goes to all Professors and staff of the Physics Department at Universidade Federal de São Carlos.

A special thanks goes to my fellow mates Caique, Marcos, and Ricardo for always being available to discuss various topics in physics and in life, and for all the fun we had over the past two years.

I would also like to thank everyone who was directly or indirectly involved in the development of this project.

Finally, I must express my profound gratitude to my parents, Fatima and Pedro, to my brother, Rodrigo, and to my sisters, Rosana and Renata, for providing me with unfailing support and continuous encouragement throughout my years of study and through the process of researching and writing this work. In special, I would like to thank my two nieces, Isadora and Iris, for bringing me the joy of life every time I go to visit them. This accomplishment would not have been possible without all of them. Thank you.

# Abstract

A system of cold bosonic atoms loaded in an optical lattice potential can undergo a macroscopic phase transition due to quantum fluctuations. As the depth of the lattice potential is increased, the ground state of the many-body system is found to go from a superfluid to a Mott-insulator state. In the presence of disorder a new phase intervenes in these transition: the Bose-glass phase. Usual analysis of this phase transition is made within the framework of mean-field theory. Such approximation predicts non-physical results for the condensate density. Taking into consideration the lack of precise analytical results in the literature, we propose the use of an effective-action approach for investigating such phase transition in the presence of disorder at arbitrary temperatures. These method, based on standard field-theoretical considerations, is used with the aim to improve the results of former analytical methods and provide better qualitative understanding of the quantum phase transition. We considered static diagonal disorder by means of a local chemical potential in the Bose-Hubbard model and obtained the phase boundary for homogeneous and Gaussian disorder distributions. We compared the condensate density predictions of our field theoretical effective-action method with the results of standard mean-field approximation. The application of the effective-action method showed to be promising in analyzing the superfluid to insulating states phase transition in the presence of disorder as well as in improving former analytical results.

**Key-words:** Effective-action. Phase-transition. Bose-glass. Insulator. Superfluid. Disorder. Bose-Hubbard model. Bose-Einstein condensation.

# Resumo

Um sistema de átomos bosônicos frios submetidos ao potencial de uma rede óptica pode sofrer uma transição de fase macroscópica devido às flutuações quânticas. À medida que a profundidade do potencial da rede é aumentada, verifica-se que o estado fundamental do sistema passa de um superfluido para um estado isolante de Mott. Na presença de desordem, uma nova fase intervém nessa transição: o vidro de Bose. A análise usual desta transição de fase é feita com o uso da teoria do campo médio. Tal aproximação apresenta resultados não físicos para a densidade de condensado do sistema. Considerando a falta de resultados analíticos precisos na literatura, propomos o uso de uma abordagem de ação efetiva para investigar essa transição de fase na presença de desordem em temperaturas arbitrárias. Esse método, baseado em considerações de teoria de campos, é usado com o objetivo de melhorar os resultados de métodos analíticos anteriores e fornecer melhor compreensão qualitativa da transição de fase quântica. Consideramos desordem diagonal estática através de um potencial químico local no modelo de Bose-Hubbard e obtivemos a linha de transição para distribuições de desordem homogênea e Gaussiana. Foram comparadas as previsões de densidade de condensado do nosso método de ação efetiva com os resultados da aproximação de campo médio. A aplicação do método da ação efetiva mostrou-se promissora na análise da transição entre superfluido e estados isolantes na presença de desordem, bem como na melhora dos resultados analíticos anteriores.

**Palavras-chave:** Ação-efetiva. Transição-de-fase. Vidro-de-Bose. Superfluido. Isolante. Desordem. Modelo-de-Bose-Hubbard. Condensado-de-Bose-Einstein.

# Contents

<b>1</b>	<b>Introduction</b>	<b>8</b>
1.1	Bose-Einstein condensation	8
1.2	Bosons in optical lattices	10
1.3	Disorder and the dirty boson problem	12
1.4	Overview	14
<b>2</b>	<b>Bosons in optical lattices</b>	<b>16</b>
2.1	Optical dipole traps	16
2.2	Single-particle properties in an optical lattice	20
2.3	Bose-Hubbard Hamiltonian	21
2.4	Hamiltonian parameters	23
<b>3</b>	<b>Quantum phase transitions</b>	<b>25</b>
3.1	Second-order quantum phase transitions	25
3.2	Landau theory	27
3.3	Mean-field approach to the superfluid-Mott insulator transition	29
<b>4</b>	<b>Effective-action approach</b>	<b>34</b>
4.1	General theory	34
4.2	Physical quantities at finite temperature	35
4.3	Perturbation theory	37
4.4	Diagrammatic representation	39
4.5	Effective action	41
4.6	Matsubara frequencies	43
4.7	Zeroth-hopping order result	44
4.8	First-hopping order result	49
<b>5</b>	<b>Disordered Bose-Hubbard model</b>	<b>51</b>
5.1	Disorder ensemble average	51
5.2	Static properties	52
5.3	Boundary between superfluid and non-superfluid phases	53
5.3.1	Pure case	54
5.3.2	Uniform homogeneous disorder distribution	54
5.3.3	Gaussian disorder distribution	56
5.4	Superfluid density	57
5.5	The Bose-glass phase	59
<b>6</b>	<b>Summary and conclusion</b>	<b>61</b>
	<b>Bibliography</b>	<b>63</b>
<b>A</b>	<b>Appendix 1</b>	<b>70</b>



# 1 Introduction

## 1.1 Bose-Einstein condensation

It is a well established fact that the motion and interaction of ordinary matter in atomic and subatomic scales can be described by the laws of quantum mechanics. When considering a system of macroscopic size, the distribution of particles in each available quantum state allows for different statistical treatments. This requires a distinction between two types of particles: bosons and fermions. The different nature of these particles gives rise to a great number of interesting physical phenomena. Identical fermions cannot occupy the same energy state, whereas identical bosons can. In fact their aggregation in the same state can even be macroscopic. Such a phenomenon was proposed by Albert Einstein in 1924 and currently still engages a substantial amount of academic research.

Using the statistical method developed by Satyendra N. Bose for the derivation of Planck's formula [1], Einstein was able to formulate the quantum theory of the monoatomic ideal gas [2,3]. According to this theory, when a gas of non-interacting bosons is cooled down to a certain critical temperature a new state of matter emerges: the Bose-Einstein Condensate (BEC). Such a state is defined as the macroscopic population of the single-particle state with zero momentum. This state was first thought unachievable given the cryogenic techniques of the time. The prediction remained of no practical use for quite a long time. In 1938, Fritz London suggested the theoretical concept of the BEC as an analogy to explain superfluidity in  $^4\text{He}$  [4]. Even though the initial theory dealt only with ideal gases, his predictions were later proved to be right [5]. The experimental realization of the BEC requires a sample so cold that the thermal de Broglie wavelength becomes larger than the mean spacing between particles. It took almost 70 years until these extremely low temperatures became experimentally accessible.

Since the beginning of the XX century the force aspect of electromagnetic radiation was experimentally confirmed, but it was only in the late 1970's that the use of this phenomenon for cooling neutral atoms was suggested. Based on such ideas, laser cooling techniques were developed during the 80's [6]. Using standing waves generated by counter-propagating lasers pointed to an atomic gas sample, one can reduce the atomic speed. If the laser frequency is red detuned below the atomic resonance frequency, an atom moving towards the light source is more likely to absorb a photon due to Doppler effect. The photon is then spontaneously emitted in a random direction by the atom. The main result of this cycle is to reduce the temperature of the atomic cloud. With the use of this technique S. Chu, C. Cohen-Tannoudji, and W. D. Phillips were able to cool atomic samples to temperatures of the order of micro-Kelvin [6–8]. For this achievement they were awarded with the physics Nobel prize in 1997 [9].

The first atomic BECs were produced in 1995 using dilute ultracold gases of alkali atoms. The choice for alkali atoms was mainly determined by the fact that their electronic transitions lie in a convenient spectral range allowing efficient manipulation by an optical laser. Such condensates were observed in gases of Rubidium by Wieman and Cornell [10], Sodium by Ketterle [11], and Lithium by Bradley [12] with the use of the laser cooling combined with an evaporative cooling technique. This method consists of successively reducing the systems trapping potential so that only the most energetic atoms can escape from the trap, thus leaving the sample colder and decreasing the temperature to the order of nano-Kelvin. Condensation was then verified using the so-called time-of-flight imaging, which consists of releasing the atomic cloud from its magnetic trap so that it can freely expand for a few milli-seconds and then taking absorption pictures (see Fig. 1). This successful experimental realization culminated in the 2001 physics Nobel prize received by Ketterle, Wieman, and Cornell [13].

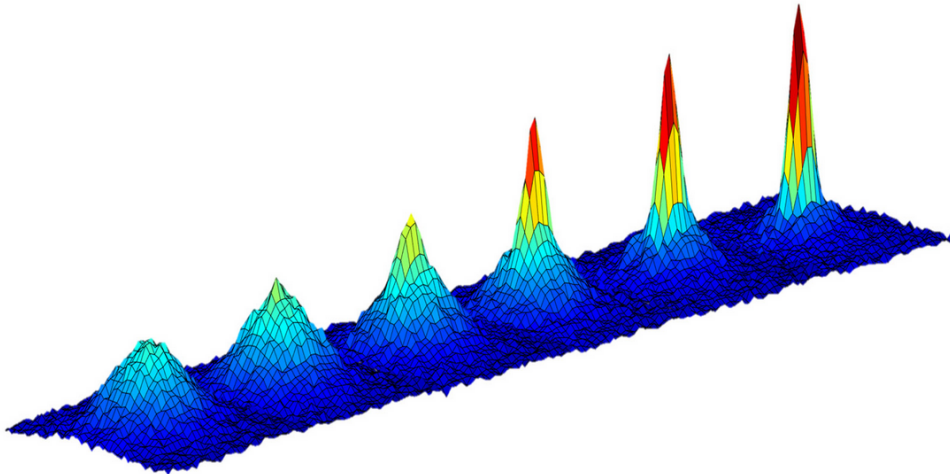


Figure 1 – The series of pictures shows the changing density of a cloud of Rubidium atoms as it is cooled down to lower and lower temperatures (form left to right) approaching absolute zero. The sharp peaks in the latter pictures indicates the formation of a BEC in this case at the temperature of 130 nano-Kelvin. Figure from Ref. [14].

After the first realization of a condensate, intense theoretical and experimental studies took place. The phenomenon of condensation turned out to play a significant role in many different fields of physics such as atomic and condensed matter physics [15]. Investigation of BECs in weakly interacting systems could lead to a better understanding of macroscopic quantum phenomena. In particular, when loaded into periodic potentials generated by laser light, the BEC atoms can be organized in structures similar to crystal lattices. Therefore, it is possible to simulate solid-state systems and also to investigate the role of interparticle interaction in the strong correlated regime, which is one of the interests of this work.

## 1.2 Bosons in optical lattices

By using counter-propagating laser beams one can create artificial crystals of light: the so-called optical lattices [16]. These electromagnetic standing waves, generated by pairs of lasers orthogonally aligned to each other, are of great use in the trapping of neutral atoms. Such waves interact with the atoms inducing an electric dipole moment. As a result, the atomic internal energy states are modified. The variation depends both on light intensity and laser frequency. The laser light is usually tuned far from atomic resonance, such that spontaneous emission can be neglected. The generated potential can be negative or positive depending on whether the laser frequency is red or blue detuned from atomic resonance, respectively. With the use of different frequencies between each pair of lasers it is possible to construct optical lattices in one [17, 18], two [19, 20], and three dimensions [20] (see Fig. 2). Lattice spacing can be controlled by changing the interference angle between the laser pairs, allowing to the creation of even triangular [21] and Kagomè structures [22].

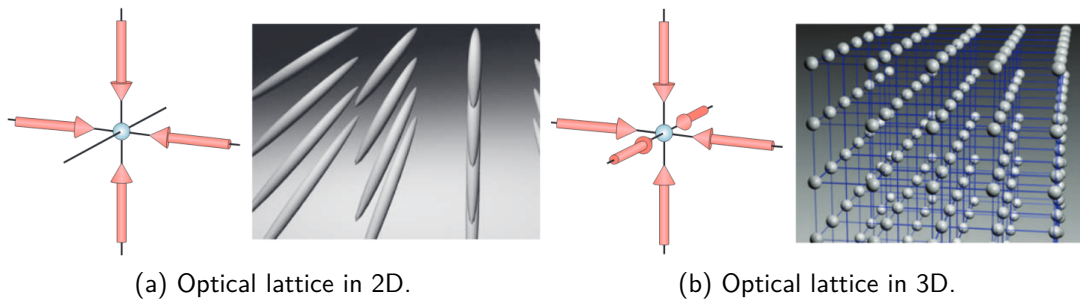


Figure 2 – Optical lattices formed by superimposing two or three pairs of orthogonal standing waves. (a) For the 2D optical lattice the atoms can move freely in one direction thus forming an array of tightly confining 1D tubes. (b) In the 3D case a simple cubic structure is built confining the atoms in attractive potentials at each lattice site. Figures from Ref. [16].

Optical lattices have been widely used as a tool to trap, cool, and control atoms. As it is free from defects and provides a fine tuning of the lattice parameters, such structures show advantages over solid-state systems to study models originally developed in condensed matter physics. One of the most interesting cases is the one of a dilute gas of bosons in the strong correlated regime. The application of a BEC loaded into an optical lattice offers a unique possibility to study fundamental questions about such regimes [23]. As the BEC is formed in temperatures of the order of nano-kelvin, the system will most probably be in the lowest energy states of the lattice wells without any need to further cooling, which makes it easier to investigate low-lying excitations. Furthermore, the raise in the density of condensates provides an increased filling factor which implies that interatomic interactions can become important [24]. The dynamics of bosons through such periodic optical potentials present similar characteristics to the motion of valence electrons in metals. By controlling the laser

intensity, the potential depth can be varied thus modifying the mobility regime of the particles and inducing in the system a quantum phase transition to a localized ground state.

Due to of the low temperatures of a BEC, for shallow lattice potentials the ground state of the weakly-interacting regime is sustained and most atoms remain condensed. When the potential depth is increased, however, the strongly-interacting regime emerges. The periodic potential changes the atom energy spectrum to a band structure. For sufficient high potential depth, transitions between Bloch bands are suppressed and the atomic cloud is confined in the lowest band. This configuration was proposed as a nearly perfect realization of the Bose-Hubbard model [25], which describes bosonic particles with repulsive interactions hopping through a lattice potential. Such model predicts a phase transition from a delocalized to a localized state. This transition was predicted by Fisher *et al.* [26] and experimentally proven by Greiner *et al.* [27].

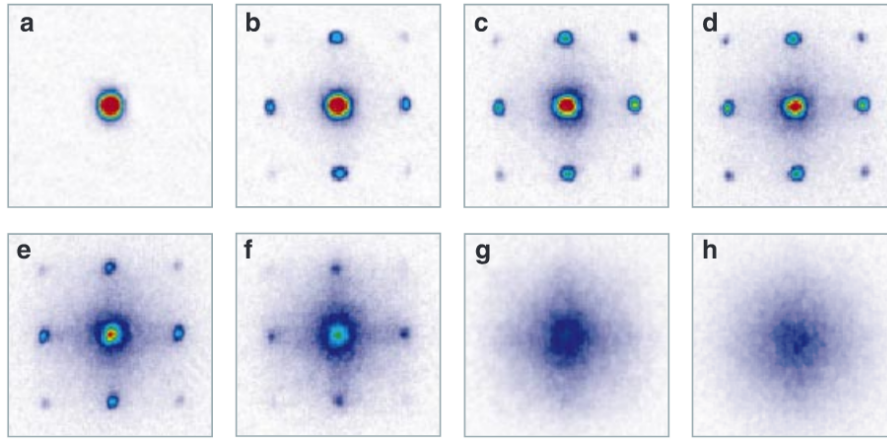


Figure 3 – Absorption pictures of multiple matter wave interference patterns obtained after releasing an ultracold gas from an optical lattice with different potential depths: (a)  $0E_r$ ; (b)  $3E_r$ ; (c)  $7E_r$ ; (d)  $10E_r$ ; (e)  $13E_r$ ; (f)  $14E_r$ ; (g)  $16E_r$ ; and (h)  $20E_r$ . Where  $E_r$  is the recoil energy which will be presented from the chapter 2. Figure from Ref. [27].

The system is characterized by two energies: the hopping energy, which is related to the probability of an atom to go from a lattice site to its neighbor by tunneling effect, and the on-site interaction energy, which accounts for interparticle interaction at the same site. If the hopping energy is greater when compared to the on-site interaction energy the atoms can move without viscosity through the system's volume and the ground state is superfluid. In the opposite case the system undergo a phase transition and a finite number of atoms becomes localized around the potential minima, which configures a Mott-insulator state. This transition can be directly tested by observing the multiple matter wave interference pattern presented in absorption images of time-of-flight measurements [23,27], as can be seen in Fig. 3. For small potential depths, perfect phase coherence can be observed, characterized by narrow interference maxima, which indicates the presence of a superfluid. As the lattice potential is

raised, the interference pattern vanishes which indicates localization in position space, thus presenting the Mott insulator regime.

Real solid-state systems generally present imperfections such as impurities or defects. As the system of a BEC in an optical lattice can be used to simulate condensed-matter models of solid-state systems, it makes sense to ask what happens when imperfections are considered. Such a case is usually addressed by means of a disordered lattice potential and allows for the emergence of a third phase other than the superfluid and Mott insulator phases, as will be discussed in the next section.

### 1.3 Disorder and the dirty boson problem

The study of a system of interacting bosonic particles in a random potential is defined in the literature as the dirty boson problem [26,28–30]. In this problem the presence of disorder along with the two-particle interaction yields an interplay between localization and superfluidity. Such disorder can appear either naturally in magnetic wire traps, where imperfections of the wire induce local disorder, or artificially by randomly adding impurity atoms of another species in the sample or even by creating a random potential using speckle laser fields [31, 32]. The experimental apparatus to the realization of the last case is sketched in Fig. 4.

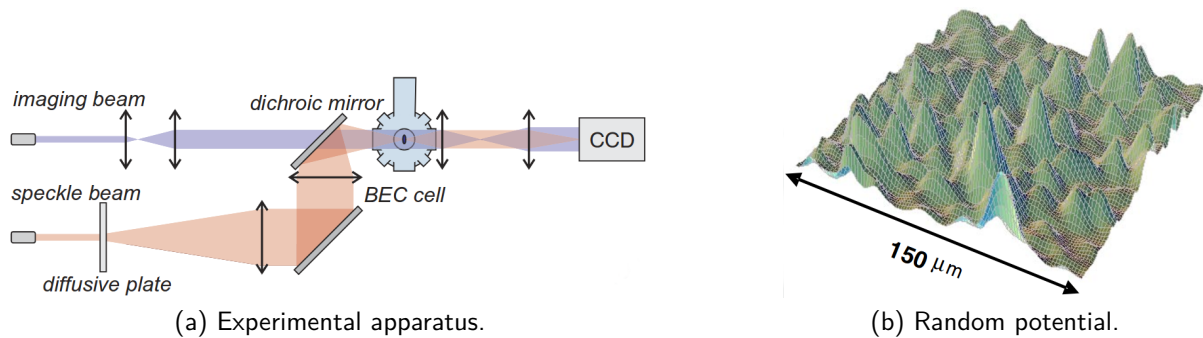


Figure 4 – Random potential experimental apparatus. (a) Optical setup for creating the speckle laser field and imaging beam for the BEC. (b) 3D representation of the disordered potential. Figure from Ref. [31].

The presence of disorder in the superfluid-Mott insulator transition gives rise to a new phase: the so-called Bose-glass phase. This phase emerges as a consequence of the competition between the hopping energy, which tries to delocalize the particles and diminish phase fluctuations, and the combined effect of interactions and random potential, which accounts for the localization of particles and reduction of density fluctuations. The theoretical prediction of such phase, made by Fisher *et al.* [26], points out that the transition to superfluidity should occur only from the Bose-glass phase. A possible phase diagram of the phase transition was proposed in the above cited paper and is shown in Fig. 5.

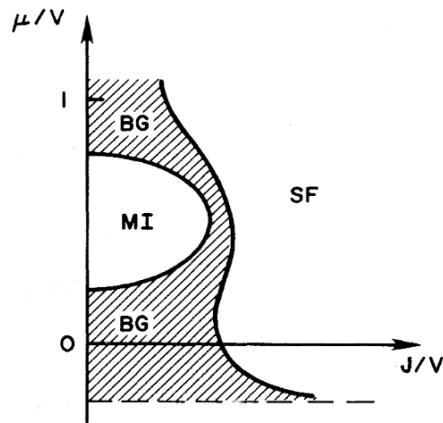


Figure 5 – Possible phase diagram for bosons in an optical lattice with weak disorder and in the zero-temperature limit. SF, BG, and MI represent the superfluid, Bose glass, and Mott insulator regions, respectively. Figure from Ref. [26].

The Bose glass is characterized as an insulating phase with continuous spectrum of excitations, showing aspects both from superfluid and insulator phases. Although some attributes of this phase are well understood, detailed information concerning the boundary of the transition are still lacking from experimental as well as theoretical point of view. Since its prediction, different studies reached contradicting conclusions about the topic [33–37]. An usual analytical investigation of this problem was made within the framework of mean-field theory [38]. This method typically fails for low dimensions and presents discrepancies when compared with high-precision Monte Carlo simulations [26,39]. The effective-action approach, developed by F.E.A dos Santos *et al.* [40–42], proved to be efficient in the analysis of the superfluid-Mott insulator transition in the absence of disorder.

The effective-action approach is constructed by using field-theoretical considerations for the inclusion of source fields in the system's Hamiltonian. Such source dependent term has a direct connection with the order parameter of interest. Perturbation theory is used to develop an expansion in the sources as well as in the hopping parameter for the theory functionals. The effective action is calculated by means of a Legendre transformation of the free energy and contains all information about the system observables regarding the superfluid and insulating phases. The results of this approach showed to be accurate when compared with high-precision simulations, with less than 3% error for the phase boundary in the 3D case, also presenting better qualitative understanding of the transition deep in the superfluid phase. Such a new theoretical method can be applied to a wide range of atomic systems in optical lattices by only adapting the Legendre transformation, which leads to the effective action, with the order parameter of the considered system [43,44]. Among other possible applications are Bose-Bose mixtures [45,46] and optical lattices with non-trivial geometries, such as triangular [21,47] and Kagomé [48].

Considering the large applicability of the effective-action approach and motivated by the lack of precise analytical methods in the literature, we propose the use of such field-theoretical method to investigate quantum phase transitions in systems consisting of BECs loaded into disordered optical potentials. In this work, we construct the general effective-action formalism and apply it to the Bose-Hubbard model by considering static diagonal disorder, which corresponds to a random chemical potential in the system's Hamiltonian. We investigate the phase boundary between superfluid and insulating states for homogeneous and Gaussian disorder distribution. Our intent is to improve the results of former analytical methods concerning the superfluid-insulator phase transition, as well as to characterize the Bose glass region on the phase diagram for both zero and finite temperatures.

## 1.4 Overview

In order to organize the discussion, we give an outline of the main points discussed here. In the first three chapters, including this introduction, we discuss some of the subjects necessary for a general comprehension of this work. The main contribution is presented in the last two chapters.

In Chapter 2, we discuss how a gas of bosonic ultracold particles can be described by the Bose-Hubbard model. We review some aspects of how the interaction of neutral particles with a laser field can be used to form optical dipole traps. The periodic part of the dipole potential is used to discuss single-particle properties in an optical lattice. The Bose-Hubbard Hamiltonian is then derived by considering a short-range s-wave scattering pseudopotential for interparticle interaction. We then calculate the Hamiltonian parameters by means of a harmonic approximation and show their dependency on the lattice potential depth. A discussion on how variations in such potential can lead to quantum phase transitions is presented.

In Chapter 3, we present a general discussion of quantum phase transitions. First, the modern classification of second-order quantum phase transition is shown. We then discuss how to use the Landau theory of phase transitions in order to obtain the phase boundary. At last we apply the mean-field theory to obtain the phase boundary for the superfluid-Mott insulator phase transition. Some limitations of this method are pointed out.

In Chapter 4, we construct the theory of the effective action. We present some arguments of the general theory and show how finite temperature quantities can be obtained. With the use of perturbation theory, we show how the important functionals of the effective-action approach can be constructed with an expansion in the hopping parameter. A diagrammatic notation is introduced to simplify further calculations. We then calculate the first-hopping order approximation for the effective action.

In Chapter 5, the effective-action approach is applied to the disordered Bose-Hubbard model. Disorder is introduced by considering a random chemical potential in the Hamiltonian.

A disorder ensemble average is used to define a homogeneous order parameter. We then calculate the disorder-averaged effective-action functional and use it to obtain the phase boundary of the superfluid to non-superfluid phase transition for homogeneous and Gaussian disorder distributions. Finally, we compare the effective-action and mean-field predictions for the condensate density in the disordered case and present how new order parameters could be introduced in order to find detailed information about each phase of the system.

In order to facilitate the comprehension, we include in Appendix 1 some details of the calculations regarding the Matsubara space expression of the correlation functions.



## 2 Bosons in optical lattices

As we have stated before, standing waves generated by pairs of lasers exert a force in each atom of the ultracold cloud thus creating the lattice structure. Neutral atoms can interact with light by both dissipative and conservative effects. Dissipative interaction is associated with the absorption of photons followed by spontaneous emission. Laser cooling techniques were developed based on this dissipative process [6]. Here we focus on the discussion of the conservative aspect the light-atom interaction. Such effect arises from the coupling between laser light and induced electric dipole moment which causes a shift in energy, called AC-Stark shift. If the detuning between light and atomic resonance is large, spontaneous emission effects can be neglected and the energy shift serves as a conservative trapping potential for bosonic neutral atoms. By considering a spatial and time dependent electric field, in the appropriate setting, the potential is approximately periodic and the single-particle solution presents a band structure. For sufficiently deep lattices the system can be described by the Bose-Hubbard model, which is the model we use to investigate quantum phase transitions in this work.

### 2.1 Optical dipole traps

We assume that the atomic wave function extends over distances much smaller than the electric field wavelength. In this configuration, the interaction can be described by the dipole approximation [49]

$$\hat{H}' = -\hat{\mathbf{d}} \cdot \boldsymbol{\mathcal{E}}, \quad (2.1)$$

where  $\boldsymbol{\mathcal{E}}$  is the electric field vector and  $\hat{\mathbf{d}}$  is the electric dipole moment operator, which has the form

$$\hat{\mathbf{d}} = -e \sum_j \hat{\mathbf{r}}_j. \quad (2.2)$$

The  $\hat{\mathbf{r}}_j$  are the position operators for the electrons with respect to the atomic nucleus and the sum runs over all electrons of the atom. In order to set the scale of effects, we begin by considering static fields. In a good approximation, atomic ground states are eigenstates of the parity operator and have even parity. Therefore, as the dipole operator is composed by position operators, in standard perturbation theory the first-order correction vanishes. The second-order approximation for static electric field is given by

$$\Delta E = - \sum_e \frac{|\langle e | \hat{H}' | g \rangle|^2}{E_e - E_g} = -\frac{1}{2} \alpha |\boldsymbol{\mathcal{E}}|^2, \quad (2.3)$$

where

$$\alpha = 2 \sum_e \frac{|\langle e | \hat{\mathbf{d}} \cdot \boldsymbol{\epsilon} | g \rangle|^2}{E_e - E_g}, \quad (2.4)$$

is the atomic polarizability, which determines the systems response to external fields, with  $\epsilon$  defined as the unity vector in the direction of the field. As usual, we label the ground state by  $g$  and the excited states by  $e$ . If we consider a two-level system, equation (2.3) simplifies to

$$\Delta E = \pm \frac{|\langle e | \hat{\mathbf{d}} \cdot \epsilon | g \rangle|^2}{E_e - E_g} |\mathcal{E}|^2, \quad (2.5)$$

for the ground and excited states. Such perturbative result obtained for the optical induced energy shift corresponds to a dipole potential. With this effect, the shifted energy could serve as a potential well which traps the atom to its minimum. This is shown in Fig. (6).

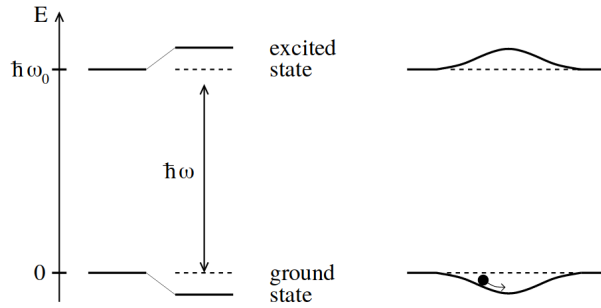


Figure 6 – Induced energy shifts for a two-level atom. In the left-hand side are the red-detuned light shifts of the ground and excited states. In the right-hand side is the ground state potential well which can be used to trap the atom. Figure from Ref. [50].

To describe the case of a time dependent electric field with frequency  $\omega$ , we write

$$\mathcal{E}(t) = \mathcal{E}_\omega e^{i\omega t} + \mathcal{E}_{-\omega} e^{-i\omega t}. \quad (2.6)$$

As such electric field is supposed to be real, the amplitudes must satisfy the following condition

$$\mathcal{E}_{-\omega} = \mathcal{E}_\omega^*. \quad (2.7)$$

With a generalization of the approach used in the static field case, one can use time-dependent perturbation theory and find the second order correction for the energy

$$\Delta E = -\frac{1}{2} \alpha(\omega) \langle |\mathcal{E}(t)|^2 \rangle_t, \quad (2.8)$$

where we define  $\langle \rangle_t$  as the time average, and the frequency dependent polarizability takes the form

$$\alpha(\omega) = 2 \sum_e \frac{(E_e - E_g) |\langle e | \hat{\mathbf{d}} \cdot \epsilon | g \rangle|^2}{(E_e - E_g)^2 - (\hbar\omega)^2}. \quad (2.9)$$

This expression differs for the static case by the shift  $\pm \hbar\omega$  in the energy denominators. In practice, only resonant transitions are considered and the term with smallest energy denominator in the polarizability dominates, which gives

$$\alpha(\omega) \approx \frac{|\langle e | \hat{\mathbf{d}} \cdot \epsilon | g \rangle|^2}{E_e - E_g - \hbar\omega}. \quad (2.10)$$

In the above calculation we implicitly assumed that the life time of the excited states was infinite, which is usually not the case. In reality an atom in an excited state will always decay to lower states by spontaneous emission of radiation. To account for this finite life time of excited states one has to calculate the rate at which this decay process occurs. This can be done by considering the relation between the Einstein coefficients of absorption and emission [51]. The inclusion of such consideration results in a complex polarizability, with the real part being responsible for the dispersive properties of the interaction while the imaginary part is related to the absorption of radiation. As we are considering absorption effects to be neglected, we focus on the real part of the polarizability, which has the form

$$\text{Re}\{\alpha(\omega)\} \approx \frac{(E_e - E_g - \hbar\omega) \left| \langle e | \hat{\mathbf{d}} \cdot \boldsymbol{\epsilon} | g \rangle \right|^2}{(E_e - E_g - \hbar\omega)^2 + (\hbar\Gamma_e/2)^2}, \quad (2.11)$$

where  $\Gamma_e$  is the rate of the decay process. The shift in energy will maintain the form of equation (2.8), and with this complex polarizability it assumes the role of an effective potential acting on the atom. This shift is usually called AC-Stark shift. Detailed information about this calculation can be found in Ref. [52].

It is convenient to express the energy shift in terms of the detuning, which is the difference between the laser frequency  $\omega$  and the frequency  $\omega_{eg} = (E_e - E_g)/\hbar$  of atomic transition

$$\delta = \omega_{eg} - \omega, \quad (2.12)$$

and the Rabi frequency, which accounts for the cycle of absorption and spontaneous emission

$$\Omega_R = \frac{1}{\hbar} \sqrt{\left| \langle e | \hat{\mathbf{d}} \cdot \boldsymbol{\mathcal{E}}_\omega | g \rangle \right|^2}. \quad (2.13)$$

The energy shift then becomes

$$\Delta E = \frac{\hbar\Omega_R^2\delta}{\delta^2 + (\hbar\Gamma_e/2)^2}. \quad (2.14)$$

For negative  $\delta$  the electric field field is tuned bellow atomic resonance. Such configuration characterizes the red detuned trap regime in which the dipole potential is negative, the interaction thus attracts the atoms into the laser field and potential minima are found with maxima light intensity. Therefore, the focal point of the laser beam already works as a stable dipole trap for the atoms. In the opposite case, above atomic resonance,  $\delta$  is positive thus constituting the blue detuned trap regime. Here the potential minima corresponds to minima light intensity and the interaction repels atoms out of the laser field. The idea of blue detuned dipole traps is to surround a spatial region with repulsive laser light.

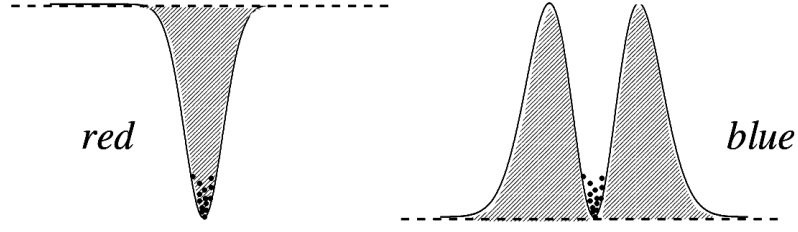


Figure 7 – Illustration of optical dipole traps with red (left) and blue (right) detuning. Figure from Ref. [50].

In order to obtain the periodic potential for the formation of optical lattices we have also to consider spatial variations in the electric field

$$\mathcal{E}(\mathbf{r}, t) = \mathcal{E}_\omega(\mathbf{r})e^{i\omega t} + \mathcal{E}_{-\omega}(\mathbf{r})e^{-i\omega t}. \quad (2.15)$$

If we take this spatial variation to be negligible inside the atoms, the interaction of laser light and induced dipole moment will generate a spatially dependent effective potential felt by each atom, which can be found in a similar manner as before with

$$V_{full}(\mathbf{r}) = -\frac{1}{2}\alpha(\omega) \langle |\mathcal{E}(\mathbf{r}, t)|^2 \rangle_t. \quad (2.16)$$

According to Ref. [53, 54], the intensity of a Gaussian laser beam is given by

$$I(\mathbf{r}) = I_0 e^{-\frac{2r^2}{\omega_0^2}} \cos^2 kz, \quad (2.17)$$

where we have considered that the laser beams are well aligned so that the beam width assumes its smallest value  $\omega_0$ . The intensity amplitude  $I_0$  depends on the electric field amplitudes. This configuration leads to a 3D potential of the form

$$V_{full}(\mathbf{r}) = -V_0 e^{-\frac{2y^2+z^2}{\omega_0^2}} \cos^2 kx - V_0 e^{-\frac{2x^2+z^2}{\omega_0^2}} \cos^2 ky - V_0 e^{-\frac{2x^2+y^2}{\omega_0^2}} \cos^2 kz, \quad (2.18)$$

which can be reorganized by considering a trap and an optical lattice part

$$V_{full}(\mathbf{r}) = V_{trap}(\mathbf{r}) + V_{OL}(\mathbf{r}), \quad (2.19)$$

with

$$V_{trap}(\mathbf{r}) = -V_0 \left( e^{-\frac{2y^2+z^2}{\omega_0^2}} + e^{-\frac{2x^2+z^2}{\omega_0^2}} + e^{-\frac{2x^2+y^2}{\omega_0^2}} \right), \quad (2.20)$$

$$V_{OL}(\mathbf{r}) = V_0 e^{-\frac{2y^2+z^2}{\omega_0^2}} \sin^2 kx + V_0 e^{-\frac{2x^2+z^2}{\omega_0^2}} \sin^2 ky + V_0 e^{-\frac{2x^2+y^2}{\omega_0^2}} \sin^2 kz.$$

Assuming that the atoms are positioned near the center of the trap, the limit  $|\mathbf{r}| \ll \omega_0$  is valid and the following approximation for the full potential can be made

$$V_{full}(\mathbf{r}) \approx -3V_0 + V(\mathbf{r}), \quad (2.21)$$

where

$$V(\mathbf{r}) = V_0(\sin^2 kx + \sin^2 ky + \sin^2 kz), \quad (2.22)$$

which is the periodic potential that will be important when analyzing the emergent band structure present in optical lattices configurations.

## 2.2 Single-particle properties in an optical lattice

We start by considering the effects of a periodic potential in the quantum state of a single particle [55]. If we consider a one dimensional potential, the Schrödinger equation takes the form

$$\left[ -\frac{\hbar^2}{2m} \frac{\partial^2}{\partial x^2} + V_0 \sin^2 kx \right] \Psi_q^{(b)}(x) = E_q^{(b)} \Psi_q^{(b)}(x), \quad (2.23)$$

where  $k$  is the laser wave number,  $b$  is the band index and  $q$  is the quasi-momentum. The potential has periodicity  $d = \lambda/2 = \pi/k$ . The solution for this equations is found by applying the Bloch theorem and representing the eigenstates in terms of periodic eigenfunctions

$$\Psi_q^{(b)}(x) = e^{iqx} \phi_q^{(b)}(x), \quad (2.24)$$

where  $\phi_q^{(b)}(x)$  has the same period as the potential. With this definition, we can see that values of  $q$  differing by  $2\pi n/d$ , with  $n$  integer, are physically equivalent, which means that the quasi-momentum can be considered to be restricted to the first Brillouin zone  $-\frac{\pi}{d} < q < \frac{\pi}{d}$ .

It is convenient to write equation (2.23) in terms of the dimensionless quantities

$$x' = \frac{\pi}{d}x, \quad q' = \frac{d}{\pi}q, \quad V_0' = \frac{V_0}{E_R} \quad \text{and} \quad \tilde{E}_q^{(b)} = \frac{E_q^{(b)}}{E_R}, \quad (2.25)$$

where  $E_R = \frac{\hbar^2 k^2}{2m}$  is the recoil energy, i.e., the energy acquired by an atom after absorbing a photon. Therefore, the dimensionless Schrödinger equation is

$$\left[ -\frac{\partial^2}{\partial x'^2} + V_0' \sin^2 x' \right] \Psi_{q'}^{(b)}(x') = \tilde{E}_{q'}^{(b)} \Psi_{q'}^{(b)}(x'). \quad (2.26)$$

By using the Bloch function representation (2.24) we get

$$\left[ q'^2 - 2iq' \frac{\partial}{\partial x'} - \frac{\partial^2}{\partial x'^2} + V_0' \sin^2 x' \right] \phi_{q'}^{(b)}(x') = \tilde{E}_{q'}^{(b)} \phi_{q'}^{(b)}(x'). \quad (2.27)$$

The periodicity of the Bloch wave  $\phi_{q'}^{(b)}(x')$  assures that a Fourier series expansion is valid

$$\phi_{q'}^{(b)}(x') = \sum_{l=-\infty}^{\infty} c_{q',l}^{(b)} e^{2ilx'}. \quad (2.28)$$

With this expansion, equation (2.27) becomes

$$\left[ (q' + 2l)^2 + \frac{V_0'}{2} \right] c_{q',l}^{(b)} + \frac{V_0'}{4} (c_{q',l+1}^{(b)} + c_{q',l-1}^{(b)}) = \tilde{E}_{q'}^{(b)} c_{q',l}^{(b)}. \quad (2.29)$$

This eigenvalue equation can be solved numerically by direct diagonalization, the solutions are shown in Fig. (8).

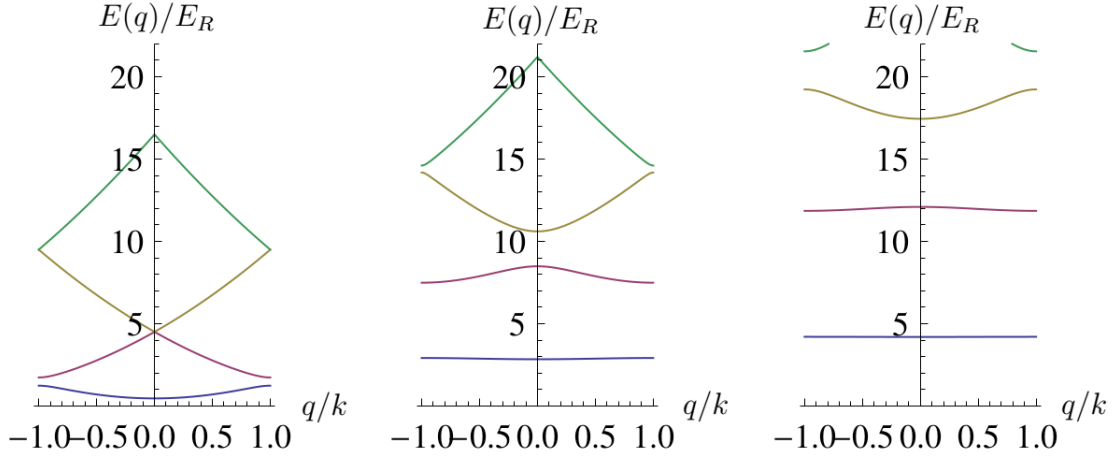


Figure 8 – Changes in the Bloch bands as the potential depth  $V'_0$  is increased. Left:  $V'_0 = 1$ . Middle:  $V'_0 = 10$ . Right:  $V'_0 = 20$ . Here  $k$  is the laser wave number and  $q$  the quasi-momentum.

The figure shows a band structure that becomes more flat as the potential depth is increased. For high enough lattice potential  $V'_0$  the energy gap between the Bloch bands increases and they become momentum independent. In the case of ultracold bosons in optical lattices, transitions between energy bands are suppressed and the atoms are considered to be confined to the lowest Bloch band, which simplifies the problem. With this, we can now turn our attention to the dynamics of such bosons through the lattice potential and derive the Bose-Hubbard Hamiltonian.

## 2.3 Bose-Hubbard Hamiltonian

An accurate description of a system composed by  $N$  identical bosons with interparticle interaction can be made with the use of the second quantization technique [56, 57]. The use of such technique simplifies the discussion of many-body systems as it already incorporates particle statistics with no need to any extra symmetrization. By considering that each particle has associated with it a single-particle Hilbert space which can be spanned by a complete set of orthonormal basis vectors, the many-body Hilbert space will be the subspace of the tensor product of these  $N$  spaces which is symmetric under the interchange of any two particles. A particularly useful basis for the construction of the many-body Hamiltonian is the basis of coordinates. For this we make use of the field creation  $\hat{\Psi}^\dagger(\mathbf{r})$  and annihilation  $\hat{\Psi}(\mathbf{r})$  operators. The Hamiltonian of a many-body system of non-relativistic interacting identical bosons with

external potential  $V(\mathbf{r})$  is given by

$$\begin{aligned} \hat{\mathcal{H}} = & \int d^3\mathbf{r} \hat{\Psi}^\dagger(\mathbf{r}) \left[ -\frac{\hbar}{2m} \nabla^2 + V(\mathbf{r}) - \mu' \right] \hat{\Psi}(\mathbf{r}) \\ & + \frac{1}{2} \int d^3\mathbf{r}_1 \int d^3\mathbf{r}_2 \hat{\Psi}^\dagger(\mathbf{r}_1) \hat{\Psi}^\dagger(\mathbf{r}_2) V_{int}(\mathbf{r}_1, \mathbf{r}_2) \hat{\Psi}(\mathbf{r}_1) \hat{\Psi}(\mathbf{r}_2), \end{aligned} \quad (2.30)$$

where  $V_{int}(\mathbf{r}_1, \mathbf{r}_2)$  is the interparticle interaction potential and  $\mu'$  denotes the grand canonical chemical potential. The field operators obey the following bosonic commutation relations

$$[\hat{\Psi}(\mathbf{r}), \hat{\Psi}^\dagger(\mathbf{r}')] = \delta(\mathbf{r} - \mathbf{r}'), \quad [\hat{\Psi}(\mathbf{r}), \hat{\Psi}(\mathbf{r}')] = 0 \quad \text{and} \quad [\hat{\Psi}^\dagger(\mathbf{r}), \hat{\Psi}^\dagger(\mathbf{r}')] = 0. \quad (2.31)$$

The interaction potential between the atoms is approximated by a short-range s-wave scattering pseudopotential [25, 58, 59]

$$V_{int}(\mathbf{r}_1, \mathbf{r}_2) = g\delta(\mathbf{r}_1 - \mathbf{r}_2) \quad \text{with} \quad g = \frac{4\pi a_s \hbar^2}{m}, \quad (2.32)$$

where  $a_s$  is the s-wave scattering length. The many-body Hamiltonian (2.30) then becomes

$$\hat{\mathcal{H}} = \int d^3\mathbf{r} \left\{ \hat{\Psi}^\dagger(\mathbf{r}) \left[ -\frac{\hbar}{2m} \nabla^2 + V(\mathbf{r}) - \mu' \right] \hat{\Psi}(\mathbf{r}) + \frac{g}{2} \hat{\Psi}^\dagger(\mathbf{r}) \hat{\Psi}^\dagger(\mathbf{r}) \hat{\Psi}(\mathbf{r}) \hat{\Psi}(\mathbf{r}) \right\}. \quad (2.33)$$

We assume that all particles are confined to the lowest Bloch band of the optical lattice. The field operator can then be expanded into a complete set of functions in the single-particle Hilbert space. In particular, we use the so-called Wannier functions  $w(\mathbf{r})$  corresponding to the periodic potential  $V(\mathbf{r})$ , which are well localized in each lattice site. For different lattice sites such functions are orthogonal, allowing a convenient basis for the expansion of the bosonic states. We can write the field operators as

$$\begin{aligned} \hat{\Psi}(\mathbf{r}) &= \sum_i \hat{a}_i w(\mathbf{r} - \mathbf{r}_i), \\ \hat{\Psi}^\dagger(\mathbf{r}) &= \sum_i \hat{a}_i^\dagger w^*(\mathbf{r} - \mathbf{r}_i), \end{aligned} \quad (2.34)$$

where  $\hat{a}_i$  and  $\hat{a}_i^\dagger$  are the bosonic annihilation and creation operators of a particle in a given lattice site. The orthogonality condition of the Wannier functions can be expressed as

$$\int_{-\infty}^{\infty} d^3\mathbf{r} w^*(\mathbf{r} - \mathbf{r}_i) w(\mathbf{r} - \mathbf{r}_j) = \delta_{ij}. \quad (2.35)$$

With the use of such condition the commutation relations for the creation and annihilation operators can be derived

$$[\hat{a}_i, \hat{a}_j^\dagger] = \delta_{ij}, \quad [\hat{a}_i, \hat{a}_j] = 0, \quad \text{and} \quad [\hat{a}_i^\dagger, \hat{a}_j^\dagger] = 0. \quad (2.36)$$

Substituting the relations (2.34) into the equation (2.33) we obtain the so-called Bose-Hubbard Hamiltonian (BHH)

$$\hat{H}_{BH} = -J \sum_{\langle ij \rangle} \hat{a}_i^\dagger \hat{a}_j + \frac{U}{2} \sum_i \hat{a}_i^\dagger \hat{a}_i^\dagger \hat{a}_i \hat{a}_i - \mu \sum_i \hat{a}_i^\dagger \hat{a}_i, \quad (2.37)$$

where the in sum  $\langle ij \rangle$  runs over all the nearest neighbors. For reasonably deep lattices, contributions due to the overlapping of Wannier functions in sites other than the nearest neighbors are negligible [59]. The explicit form of the BHH parameters is given by

$$\begin{aligned} J &= \int d^3\mathbf{r} w^*(\mathbf{r} - \mathbf{r}_i) \left[ -\frac{\hbar^2}{2m} \nabla^2 + V(\mathbf{r}) \right] w(\mathbf{r} - \mathbf{r}_j), \\ U &= g \int d^3\mathbf{r} |w(\mathbf{r})|^4, \\ \mu &= \mu' - \int d^3\mathbf{r} w^*(\mathbf{r}) \left[ -\frac{\hbar^2}{2m} \nabla^2 + V(\mathbf{r}) \right] w(\mathbf{r}). \end{aligned} \quad (2.38)$$

The BHH describes the physics of bosonic particles hopping through a lattice. The hopping energy  $J$  is associated with the probability of a particle to hop from a lattice site to its neighbor by tunnel effect and the on-site interaction  $U$  is responsible for the interparticle interaction at the same lattice site. In this sense, a particle gains energy proportional to  $J$  by hopping from one lattice site to the next while particles occupying the same site feel the mutual interaction  $U$ . The chemical potential  $\mu$  controls the number of particles in the grand canonical ensemble. Variations in the lattice potential depth can change the relation between these parameters. Direct calculation of such parameters is presented in the next section.

## 2.4 Hamiltonian parameters

A qualitative insight into the dependence of the BHH parameters can be obtained with a harmonic approximation, expanding around the minima of each potential well [60]. The Wannier functions then factorize in the product of harmonic oscillator states in each direction, which makes it possible to look at the problem in one dimension. In this harmonic approximation, the one dimensional Schrödinger equation for the Wannier function is given by

$$\left[ -\frac{\hbar^2}{2m} \frac{\partial^2}{\partial x^2} + V_0 k^2 x^2 \right] w(x) = E w(x). \quad (2.39)$$

In each lattice potential well, the ground state solution for the Wannier function is

$$w(x) = \left( \frac{k\sqrt{2V_0m}}{\pi\hbar} \right)^{\frac{1}{4}} \exp \left[ -\frac{k\sqrt{2V_0m}}{2\hbar} x^2 \right], \quad (2.40)$$

or, in dimensionless unities (2.25)

$$w(x) = \left( \frac{\pi\sqrt{V'_0}}{d^2} \right)^{\frac{1}{4}} \exp \left[ -\frac{\pi\sqrt{V'_0}}{2} \left( \frac{x}{d} \right)^2 \right]. \quad (2.41)$$

From this ground state solution all the parameters can be approximated by applying it to the relations shown in (2.38).



For reasonably deep lattice potentials,  $V_0 \gtrsim 5E_R$  [59], the result of the integration is

$$\begin{aligned}
 J &= E_R V_0' \left( \frac{\pi^2}{4} - 1 \right) \exp \left[ -\frac{\pi^2}{4} \sqrt{V_0'} \right], \\
 U &= \sqrt{8\pi} \frac{E_R a_s}{d} (V_0')^{\frac{3}{4}}, \\
 \mu &= \mu' - 3E_R \sqrt{V_0'}.
 \end{aligned} \tag{2.42}$$

Such results show that variations on the lattice potential depth will change the interplay between the Hamiltonian parameters, which indicates a transition in the regime of movement of the particles. For deep lattice potentials the barriers between lattice sites is increased thus leading to vanishing hopping energy  $J$ . However, this process makes particles occupying the same site more compressed and the repulsive interaction energy  $U$  is increased. This situation can be explored by means of the theory of quantum phase transitions which is presented in the next chapter.

## 3 Quantum phase transitions

One important facet of bosonic particles in optical lattices is related to the study of quantum phase transitions. Here, we present a general introduction of the theory of second-order quantum phase transitions according to the modern classification. Such transitions are driven by quantum fluctuations and are possible even at the zero-temperature limit. The concept of spontaneous symmetry breaking during phase transition and the role of an order parameter are discussed by means of the Landau theory. The order parameter is used to construct an expansion for the thermodynamic potential which presents different properties in each phase. The phase diagram for the superfluid-Mott insulator transition is obtained with the use of a mean-field theory. Properties of these two phases are addressed and limitations of the mean-field approximation are pointed out.

### 3.1 Second-order quantum phase transitions

Phase transition is the term used to characterize the description of the transition of a macroscopic system from one state of matter to another. During such physical phenomena, certain properties of the medium change, as a result of the variation of some external condition. A familiar example would be water boiling to steam, where the liquid water becomes a gas upon heating, which leads to an abrupt change in volume. The main external condition responsible for the transition in this example is the change in temperature, however, phase transitions can occur due to pressure variation or even due to the presence of external electric or magnetic fields. To obtain a more general definition of a phase transition it is often useful to map some of these external conditions into control parameters of the underlying Hamiltonian of the given system. The use of such parameters makes it possible to define a phase boundary in the control parameter space. A precise classification of a phase transition comes from the analysis of the behavior of thermodynamic functions in such space [61]. Precisely, phase transitions are defined as points in the parameter space where thermodynamic functions of the given system present singularities.

In principle, for a finite system, singularities may never arise from the partition function, as it is composed of a finite sum of analytical functions, therefore, always analytic. Singular behavior of the partition function is made possible when the system's size together with its number of particles are considered to be infinite. Such consideration is known as the *thermodynamic limit* [62], which is usually a good approximation as macroscopic systems typically contain particle number of the order of  $10^{23}$ . As we approach this limit, singularities in the partition function may emerge. To understand the role of non-analycity in phase transitions it is convenient look at the behavior of the thermodynamic potential, as such

function represents the thermodynamic state of the system. The modern classification of phase transitions is based on the analysis of whether the thermodynamic potential varies continuously or not during the transition.

Transitions that present a discontinuous thermodynamic potential are associated with latent heat and are called first-order phase transitions. Examples would be solid-liquid and liquid-gas transitions. If the thermodynamic potential varies continuously at the transition point, no latent heat is involved and we are in the domain of a continuous or second-order phase transitions. An example of such transition would be a ferromagnetic-paramagnetic phase transition. A point in the phase diagram where a second-order phase transition takes place is called *critical point*. Non-analyticity near second-order phase transitions characterize the so-called *critical phenomena*. Here, our main interest will be in second order quantum phase transitions.

Unlike classical phase transitions, which are induced by a change in temperature, quantum phase transitions are driven by quantum fluctuations. Therefore, such transitions are allowed even at the zero-temperature limit. These quantum fluctuations can be interpreted as non-analyticities in the ground-state energy of the given system [63], where a competition between control parameters of the system's Hamiltonian takes place. If for sake of simplicity we consider a Hamiltonian,  $H(g)$ , whose degrees of freedom reside on the sites of a lattice and which varies as function of a dimensionless coupling  $g$ , we can observe the evolution of the ground state energy. If  $g$  couples only to a conserved quantity, we can write  $H(g) = H_0 + gH_1$ , where  $H_0$  and  $H_1$  commute. Such description assures the possibility of level crossing where an excited state becomes the ground state when  $g = g_c$ , creating a point of non-analyticity in the ground state energy. More generally, an avoided level crossing becomes sharper as the lattice size increases, thus leading to non-analyticity in the infinite lattice limit (see Fig. (9)).

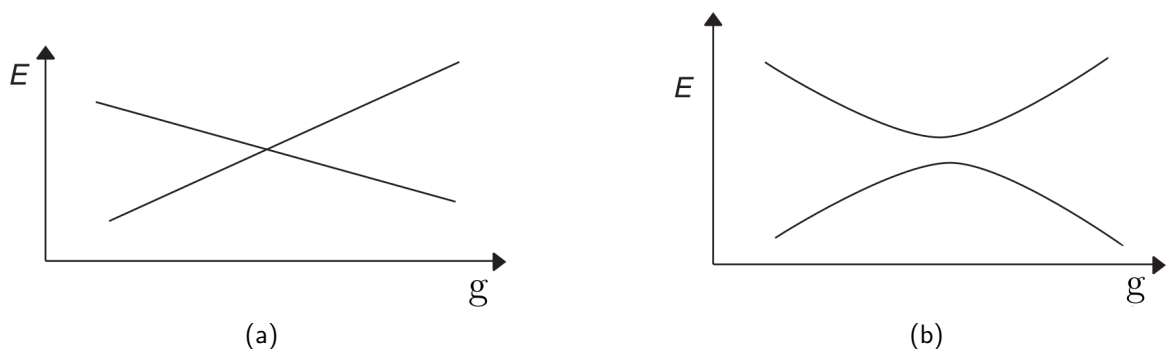


Figure 9 – Low eigenvalues,  $E$ , of the Hamiltonian  $H(g)$  as a function of  $g$  on a finite lattice. In (a) we see the actual level-crossing and in (b) the more general case of an avoided level-crossing. Figure from Ref. [63].

Second-order quantum phase transitions can be interpreted as transitions where the characteristic energy scale of fluctuations vanishes as  $g$  approaches  $g_c$ . The singular behavior

of the energy of the lowest excitation above the ground state  $\Delta E$  is assumed to be proportional to some power of  $g - g_c$  in the zero temperature limit. In the phase boundary, i.e.  $g \rightarrow g_c$ , scaling theory predicts

$$\Delta E \sim \mathcal{J}|g - g_c|^{3\nu}, \quad (3.1)$$

where  $\mathcal{J}$  is the energy scale of characteristic microscopic coupling and  $3\nu$  is a *critical exponent*. The value of  $3\nu$  is independent of microscopic details of the Hamiltonian and is said to be *universal*. If  $\Delta E$  is nonzero, the energy spectrum has a gap. In the other hand, if there are excitations with arbitrarily low energies in the limit of infinite lattice the spectrum is said to be *gapless*.

Phase transitions usually change the nature of correlations in the ground state. Along with a vanishing energy scale, second-order quantum phase transitions present a divergent correlation length  $\xi$ . Such divergence can be described in a similar manner as before by

$$\xi^{-1} \sim \Lambda|g - g_c|^\nu, \quad (3.2)$$

where  $\nu$  is another critical exponent and  $\Lambda$  is an inverse length scale of the order of the inverse lattice spacing. Comparing equations (3.1) and (3.2), we see that

$$\Delta E \sim \xi^{-3}. \quad (3.3)$$

From this relation we can see that as the characteristic length scale  $\xi$  diverges, the energy gap  $\Delta E$  vanishes, which is in agreement with our definition of second-order phase transition. The exponent  $3$  is called the dynamic critical exponent. Although this formulation was made in the zero-temperature limit, it turns out that it also serves as a powerful way to describe dynamic and thermodynamic properties of systems near phase transition even for finite temperatures.

## 3.2 Landau theory

Throughout a phase transition, the symmetry presented by one of the phases may be reduced when the phase boundary is crossed and the other phase is reached. In 1937 Lev Landau introduced the concept of a broken symmetry to explain second-order phase transitions [64, 65]. He introduced an extra unique thermodynamic variable to describe the system in the less symmetrical phase: the *order parameter*. Such parameter represents the degree of order across the phase boundary and it normally ranges from zero in the symmetric phase to a non-zero value in the less symmetric one. The choice for this order parameter is made by considering its utility. Well-known examples would be the spontaneous magnetization for paramagnetic-ferromagnetic transition or the difference of the densities for liquid-gas transitions.

As Bose-Einstein condensation implies phase coherence [15], a convenient choice for the order parameter of a BEC would be the macroscopic wave function of the condensate

$\Psi(\mathbf{r}) = \langle \hat{\Psi}(\mathbf{r}) \rangle$ . In the last chapter we argued that the low-temperature physics of spinless bosons loaded in optical lattices may be well described by the single-band BHH. In this case, the order parameter can be similarly defined as  $\psi_i = \langle \hat{a}_i \rangle$  or just  $\psi$  if the system is assumed to be homogeneous. In the ordered phase, the order parameter must assume some value  $\psi = Ae^{i\theta}$ , with a well defined value for  $\theta$ , while in the disordered phase we have  $\psi = 0$ . In principle, the condensate wave function's phase  $\theta$  is unknown, however, the ordered phase is only achieved by spontaneous symmetry breaking when such quantity assumes a specific value. This direction for  $\theta$  is in practice decided by infinitesimal external perturbations such as boundary conditions.

Without any external perturbation, the set of values for the phase  $\theta$  correspond to a global U(1) symmetry in the BHH. Each possible value of  $\theta$  is associated with a set of microscopic configurations of the system that have the same energy. According to Boltzmann's ergodic hypothesis, as time progresses the system passes from one configuration to another and will eventually visit all microscopic configurations. For a large system, however, the time for it to visit the whole set of configurations may become infinite. Therefore, the system may not be able to explore the whole configuration space and becomes confined to a subspace which corresponds to  $\psi = Ae^{i\theta}$ . Thus, spontaneous symmetry breaking is achieved dynamically as a result of *ergodicity breaking*.

For the Landau theory, the central actor is the free-energy functional  $\mathcal{F}$ , which has to be minimized with respect to variations of  $\psi$ . This can be expressed as

$$\frac{\partial \mathcal{F}}{\partial \psi} = 0 \quad , \quad \frac{\partial \mathcal{F}}{\partial \psi^*} = 0. \quad (3.4)$$

The minimization of  $\mathcal{F}$  is equivalent to the maximization of the entropy of the system. As consequence of the global symmetry of the BHH the free energy must be invariant under phase rotations of the order parameter  $\psi$ . This implies that  $\mathcal{F}$  must be a function of  $|\psi|^2$ . The order parameter increases continuously from zero when the ordered phase is reached. Near the phase boundary its value is small, thus a good approximation for the free energy would be the first few terms of the Taylor expansion in the order parameter

$$\mathcal{F} = a_0 + a_2|\psi|^2 + a_4|\psi|^4 + \dots . \quad (3.5)$$

According to this theory, second order phase transitions may be fully explained by only considering the coefficients  $a_2$  and  $a_4$ . Equation (3.4) together with (3.5) gives the absolute value of the order parameter at the vicinity of the phase boundary

$$|\psi| = \sqrt{-\frac{a_2}{2a_4}}. \quad (3.6)$$

If we take  $a_4$  to be positive, the phase transitions is characterized by a change in the sign of  $a_2$  (see Fig. (10)).

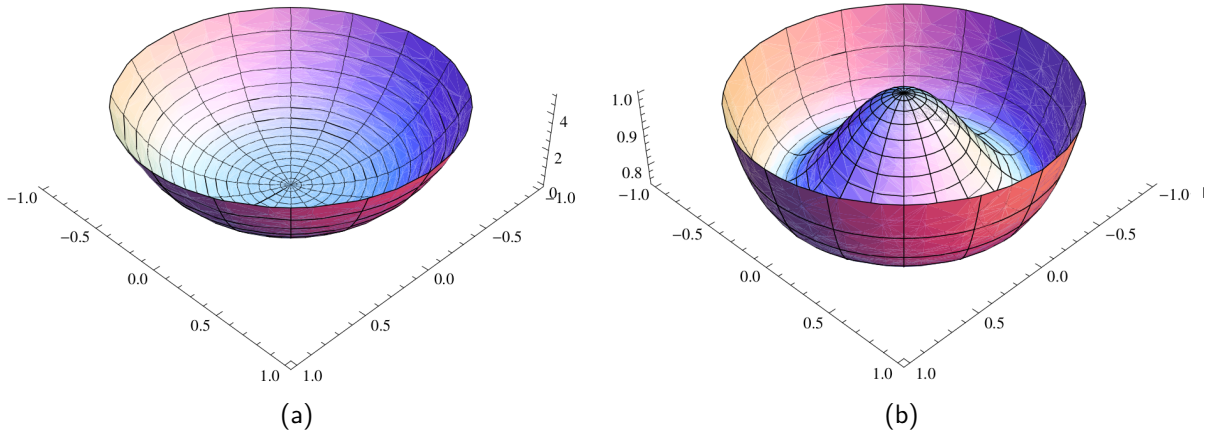


Figure 10 – Landau free energy functional. Figure (a) shows a single minimum potential which characterizes the symmetric phase. Figure (b) show a Mexican-hat potential typical in a symmetry-broken phase.

If  $a_2 > 0$  the only solution for equation (3.6) is  $\psi = 0$ , thus leading to a symmetric phase. In the opposite case, for  $a_2 < 0$ , the free energy presents infinitely many minima with  $\psi \neq 0$  each one with a different phase  $\theta$ , which characterizes the symmetry-broken phase. Therefore, the condition  $a_2 = 0$  defines the phase boundary between ordered and disordered phases in the control parameter space.

### 3.3 Mean-field approach to the superfluid-Mott insulator transition

By considering the number operator  $\hat{n}_i = \hat{a}_i^\dagger \hat{a}_i$  we can re-write the BHH in equation (2.37) in the following form

$$\hat{H}_{BH} = \frac{U}{2} \sum_i \hat{n}_i (\hat{n}_i - 1) - \mu \sum_i \hat{n}_i - J \sum_{\langle ij \rangle} \hat{a}_i^\dagger \hat{a}_j. \quad (3.7)$$

Here, we consider the zero-temperature limit. The non-local hopping term makes it difficult for a direct solution. This problem can be simplified by means of a mean-field approach. Such method consists of an approximation of the boson creation and annihilation operators by their expectation values

$$\hat{a}_i = \langle \hat{a}_i \rangle + \delta \hat{a}_i, \quad \hat{a}_i^\dagger = \langle \hat{a}_i^\dagger \rangle + \delta \hat{a}_i^\dagger. \quad (3.8)$$

With this relations the hopping term can be expanded as

$$-J \sum_{\langle ij \rangle} \hat{a}_i^\dagger \hat{a}_j = -J \sum_{\langle ij \rangle} \left( \langle \hat{a}_i^\dagger \rangle \langle \hat{a}_j \rangle + \langle \hat{a}_i^\dagger \rangle \delta \hat{a}_j + \delta \hat{a}_i^\dagger \langle \hat{a}_j \rangle + \delta \hat{a}_i^\dagger \delta \hat{a}_j \right). \quad (3.9)$$

If we neglect products of fluctuations, i.e., neglect the term  $\delta \hat{a}_i^\dagger \delta \hat{a}_j$ , and assume homogeneity of the system, which means  $\langle \hat{a}_i \rangle = \psi$  and  $\langle \hat{a}_j^\dagger \rangle = \psi^*$ , the hopping term takes the simpler form

$$-J \sum_{\langle ij \rangle} \hat{a}_i^\dagger \hat{a}_j \approx -Jz \sum_i \left( \psi^* \hat{a}_i + \hat{a}_i^\dagger \psi - \psi^* \psi \right), \quad (3.10)$$

where  $z$  is the number of nearest neighbors. Such approximation makes it possible to obtain the mean-field Hamiltonian

$$\hat{H}_{MF} = \frac{U}{2} \sum_i \hat{n}_i(\hat{n}_i - 1) - \mu \sum_i \hat{n}_i - Jz \sum_i (\psi^* \hat{a}_i + \hat{a}_i^\dagger \psi - \psi^* \psi). \quad (3.11)$$

Due to the homogeneity assumption the order parameter is site independent, which implies that translational symmetry is not broken. Our analysis is thus much simpler as the problem is described as a set of identical independent Hamiltonians one for each lattice site. The mean-field Hamiltonian  $\hat{H}_{MF}$  does not present an explicit global U(1) symmetry as does the BHH, which is necessary for the emergence of a symmetry-broken phase. However, if we treat the new hopping term as a perturbation, the ground state energy must still present phase invariance in the order parameter and can be expanded as a Landau series

$$\frac{E_{MF}(|\psi|^2)}{N_s} = a_0 + a_2 |\psi|^2 + a_4 |\psi|^4 + \dots, \quad (3.12)$$

where  $N_s$  is the total number of lattice sites,  $a_0$  is the ground state energy of the BHH for the case of  $J = 0$  and the two coefficients  $a_2$  and  $a_4$  can be calculated by Rayleigh-Schrödinger perturbation theory. The unperturbed part of the Hamiltonian is

$$\hat{H}_0 = \frac{U}{2} \hat{n}(\hat{n} - 1) - \mu \hat{n}, \quad (3.13)$$

where we ignored the site index as all sites are equivalent. This Hamiltonian depends only on the number operator, thus its eigenstates contain an integer number of bosons per lattice site and the eigenvalues are given by

$$f_n = \frac{U}{2} n(n - 1) - \mu n. \quad (3.14)$$

Comparing different eigenvalues, we see that the  $n$  which minimizes the unperturbed energy has the form

$$n\left(\frac{\mu}{U}\right) = 1 + \text{int}\left(\frac{\mu}{U}\right), \quad (3.15)$$

where  $\text{int}\left(\frac{\mu}{U}\right)$  stands for the integer part of  $\frac{\mu}{U}$ . Applying time-independent second-order perturbation theory to the hopping term in the mean-field Hamiltonian, we obtain

$$\begin{aligned} a_0 &= f_n, \\ a_2 &= Jz + (Jz)^2 \left( \frac{n+1}{f_n - f_{n+1}} + \frac{n}{f_n - f_{n-1}} \right), \\ a_4 &= (Jz)^4 \left( \frac{(n+2)(n+1)}{(f_n - f_{n+1})^2 (f_n - f_{n+2})} - \frac{n(n-1)}{(f_n - f_{n-1})^2 (f_n - f_{n-2})} \right) \\ &\quad - (Jz)^4 \left( \frac{n+1}{(f_n - f_{n+1})^2} + \frac{n}{(f_n - f_{n-1})^2} \right) \left( \frac{n+1}{f_n - f_{n+1}} + \frac{n}{f_n - f_{n-1}} \right). \end{aligned} \quad (3.16)$$

We calculate the phase boundary by imposing the condition  $a_2 = 0$ , which leads to

$$\frac{Jz}{U} = \frac{(n - \mu/U)(\mu/U - n + 1)}{1 + \mu/U}. \quad (3.17)$$

The phase diagram is depicted in Fig. 11. Such diagram shows a series of lobes, each one corresponding to an occupation number  $n$ . Inside these lobes the particle density is constant, which implies that they are Mott-insulator phases. Outside of this region the order parameter becomes non-zero indicating the emergence of a macroscopic wave function, which corresponds to a BEC. As a consequence of the existence of such wave function, a fraction of the system moves without viscosity through the lattice characterizing a superfluid phase. Using a relation analogous to the equation (3.6) for the mean-field energy minimization near the phase boundary but still in the superfluid phase we can define  $|\psi_{MF}|^2 = -\frac{a_2}{2a_4}$  as the condensate density as it accounts for the density of particles sharing the condensate wave function.

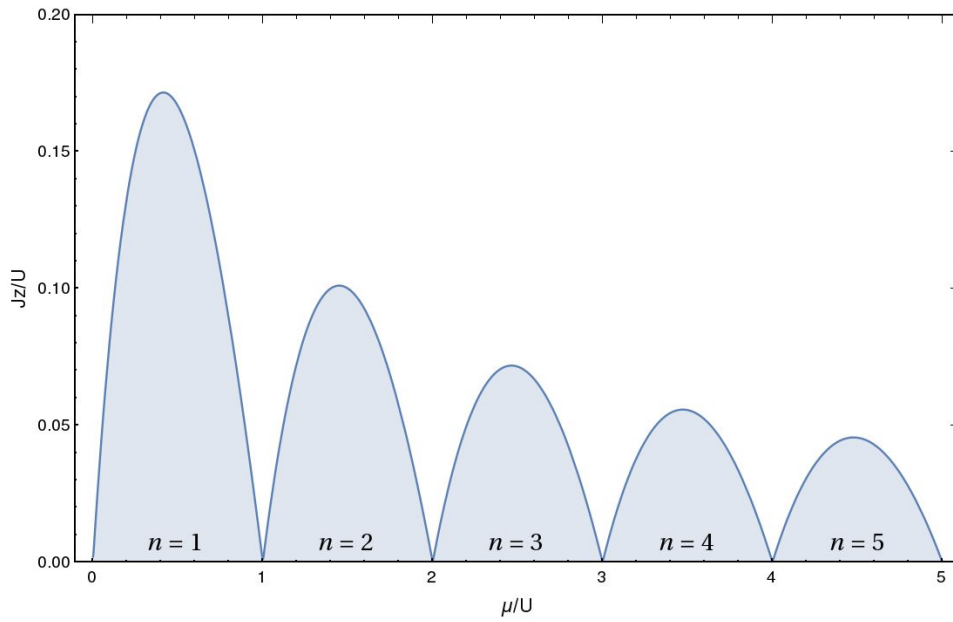


Figure 11 – Mean field quantum phase diagram for the Bose-Hubbard model. The filled blue region corresponds to successive Mott lobes each associated to an integer occupation number  $n$ . Outside of this lobes is the superfluid region.

The critical point for the transition from a superfluid to a Mott insulator state with an integer number of particles  $n$  is given by the ratio  $J/U$  at the up border of the graph. A large chemical potential will reveal further lobes representing Mott-insulator states with higher occupation numbers. The Mott-insulator state opens up an energy gap in the spectrum of excitations [23]. As discussed in the previous section, scaling theory shows [26] that close to the critical point this gap vanishes as

$$\Delta E \sim \left( \left( \frac{J}{U} \right)_c - \frac{J}{U} \right)^{\beta\nu}. \quad (3.18)$$

These mean-field approach yields  $\beta\nu = 1/2$  [23, 66].

The result obtained through the mean-field theory allows for the calculation of the superfluid density. This quantity is defined as the effective fluid density that remains at rest



when the entire system is moved at constant velocity [67]. We can calculate the superfluid density introducing a Galilei boost [40, 68]

$$E(\boldsymbol{\phi}) = E(\mathbf{0}) + \frac{1}{2}\rho_s N_s m \boldsymbol{v}^2, \quad (3.19)$$

with  $E(\boldsymbol{\phi})$  being boosted energy,  $E(\mathbf{0})$  the energy without the boost,  $\rho_s$  the superfluid density,  $m$  the effective particle mass, and  $\boldsymbol{v}$  the velocity. The vector  $\boldsymbol{\phi}$  is related to the velocity in the following way

$$\boldsymbol{v} = \frac{\hbar}{mL}\boldsymbol{\phi}, \quad (3.20)$$

where  $L$  is the systems extent in the velocity direction. Equivalently, we can add the Peierls phase factor to the bosonic operator

$$\hat{a}_j \rightarrow \hat{a}_j e^{ir_j \cdot \boldsymbol{\phi}/L}. \quad (3.21)$$

The superfluid density is then defined as

$$\rho_s = \lim_{|\boldsymbol{\phi}| \rightarrow 0} \frac{2L^2}{N_s J d^2 |\boldsymbol{\phi}|^2} [E(\boldsymbol{\phi}) - E(\mathbf{0})]. \quad (3.22)$$

As shown in Ref. [68], in the mean-field approximation the superfluid density has exactly the same value as the condensate density. Fig. 12 shows such density for different values of the chemical potential.

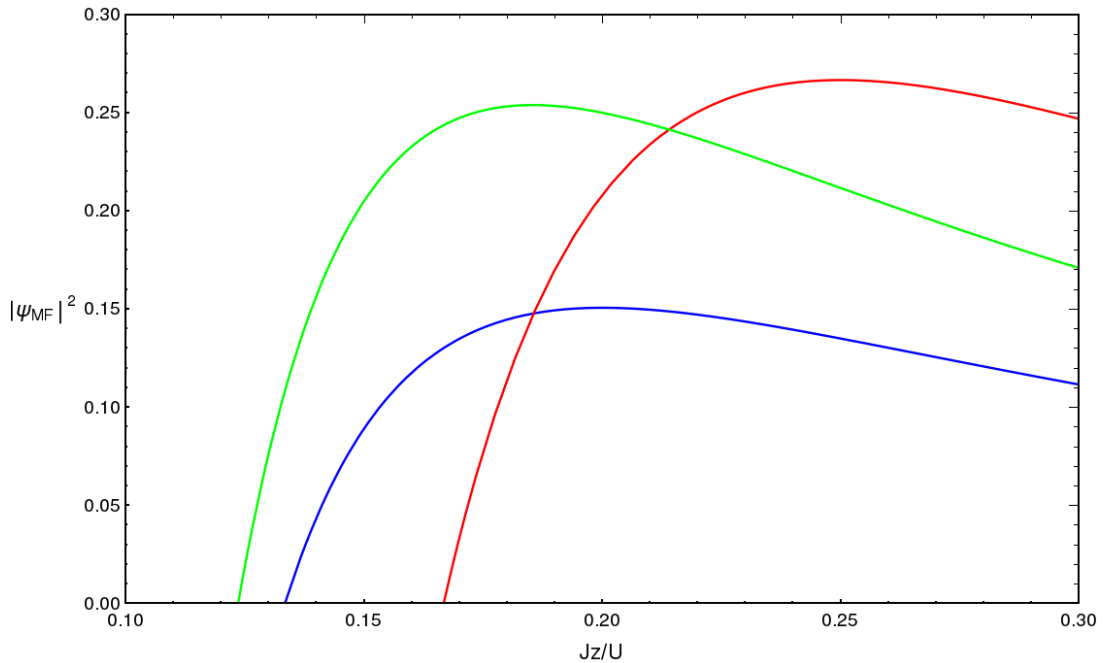


Figure 12 – Mean field condensate/superfluid density as a function of the hopping parameter. The blue, red, and green lines correspond to  $\mu/U = 0.2$ ,  $\mu/U = 0.5$  and  $\mu/U = 0.7$ , respectively.

As the hopping parameter goes deeper in the superfluid phase, we would expect an increase in the condensate density. We can see that the mean-field result predicts an

non-physical behavior for such quantity. These limitations of the mean-field theory were pointed out in Ref. [41,42], where it was also shown that such theory predicts a non-physical compressibility. In addition, the approximations are too restrictive, thus eliminating any difference between superfluid and condensate density. In order to improve these analytical results one can use field-theoretical considerations and apply an effective-action approach. The construction of this method is shown in the next chapter.

## 4 Effective-action approach

In this chapter we use quantum field theory arguments to derive a Landau expansion for an effective action with a spatially and temporally independent global order parameter, thus defining the effective potential. This function encloses all information necessary to study quantum phase transitions at zero and arbitrary temperatures. In particular, we use the Bose-Hubbard model in order to construct such a function as a Taylor expansion of the hopping parameter. In order to simplify our calculations, a diagrammatic notation is introduced, which facilitates the computation of high-order terms in the hopping expansion. We use such representation to obtain all effective-action terms needed to our investigation of the superfluid-insulator transition in the presence of disorder. The calculations presented in this chapter follow the ideas from Ref. [40–42], where detailed information can be found.

### 4.1 General theory

So far we have discussed second-order quantum phase transitions where the global U(1) symmetry is broken with the assumption of a homogeneous order parameter. This approach is not valid for dealing with phase transitions which also present translational symmetry breaking, where we would have a site-dependent order parameter. Therefore, in order to take this non-homogeneity into consideration, we must introduce to our analysis site-dependent sources, which lead to a more general thermodynamic potential. The site-dependent sources  $j_i$  and  $j_i^*$  impose the constraint  $\langle \hat{a}_i \rangle = \psi_i$  and  $\langle \hat{a}_i^\dagger \rangle = \psi_i^*$ . An even broader theory would be accomplished by means of an analogy between the quantum-mechanical time evolution operator and the quantum-statistical density matrix. If we consider  $\hbar = 1$ , the evolution operator  $e^{-it\hat{H}}$  shows the same form of the operator  $e^{-\beta\hat{H}}$ , which can be thought of as a quantum-evolution operator evolving in imaginary time from 0 to  $\beta$  with a Wick rotation  $\tau \rightarrow it$ . With this general field theoretical considerations [69, 70], the study of the system near a second-order quantum phase transition can be made by introducing to the Hamiltonian site-dependent as well as imaginary-time dependent sources  $j_i(\tau)$  and  $j_i^*(\tau)$

$$\hat{H}_{BH}(\tau) = \hat{H}_{BH} + \sum_i [j_i^*(\tau)\hat{a}_i + j_i(\tau)\hat{a}_i^\dagger]. \quad (4.1)$$

The introduction of such sources is artificially made with the intention of explicitly breaking any global symmetries.

In order to find a perturbative expression for the grand canonical free energy, we notice that the imaginary-time evolution operator obeys the following equation

$$-\frac{\partial \hat{U}(\tau, \tau_0)}{\partial \tau} = \hat{H}_{BH}(\tau)\hat{U}(\tau, \tau_0), \quad (4.2)$$

where  $\hat{U}(\tau_0, \tau_0) = 1$ . The solution for this differential equation can be expressed as

$$\hat{U}(\tau, \tau_0) = \hat{T} \left\{ \exp \left[ - \int_{\tau_0}^{\tau} d\tau' \hat{H}_{BH}(\tau') \right] \right\}, \quad (4.3)$$

where  $\hat{T}$  stands for the time-ordering operator. The generalized source-dependent grand canonical partition function is then defined as

$$Z[j_i^*(\tau), j_i(\tau)] = \text{Tr} [\hat{U}(\beta, 0)]. \quad (4.4)$$

With this quantity, we are able to obtain the free-energy functional

$$F[j_i^*(\tau), j_i(\tau)] = -\frac{1}{\beta} \ln \{ Z[j_i^*(\tau), j_i(\tau)] \}. \quad (4.5)$$

A more general investigation of phase transitions can be made through this free-energy functional. In addition, physical quantities may be found by taking functional derivatives of  $F$  with respect to the sources. In particular, the order parameters are given by

$$\psi_i(\tau) = \langle \hat{a}_i(\tau) \rangle = \beta \frac{\delta F[j_i^*(\tau), j_i(\tau)]}{\delta j_i^*(\tau)}, \quad \psi_i^*(\tau) = \langle \hat{a}_i^\dagger(\tau) \rangle = \beta \frac{\delta F[j_i^*(\tau), j_i(\tau)]}{\delta j_i(\tau)}. \quad (4.6)$$

By means of a Legendre transformation of the free energy, we find the effective action which depends on the order parameter field

$$\Gamma[\psi_i^*(\tau), \psi_i(\tau)] = F - \frac{1}{\beta} \sum_i \int_0^\beta d\tau [\psi_i^*(\tau) j_i(\tau) + \psi_i(\tau) j_i^*(\tau)]. \quad (4.7)$$

Once we observe that the real physical situation of interest corresponds to the case where the artificially introduced sources vanishes,  $j_i(\tau) = j_i^*(\tau) = 0$ , the importance of the effective action is understood. As  $j$  and  $\psi^*$  are conjugate variables, we must have

$$j_i(\tau) = \beta \frac{\delta \Gamma[\psi_i^*(\tau), \psi_i(\tau)]}{\delta \psi_i^*(\tau)} \quad \text{and} \quad j_i^*(\tau) = \beta \frac{\delta \Gamma[\psi_i^*(\tau), \psi_i(\tau)]}{\delta \psi_i(\tau)}, \quad (4.8)$$

thus the physical situation is obtained for

$$\frac{\delta \Gamma[\psi_i^*(\tau), \psi_i(\tau)]}{\delta \psi_i^*(\tau)} = 0 \quad \text{and} \quad \frac{\delta \Gamma[\psi_i^*(\tau), \psi_i(\tau)]}{\delta \psi_i(\tau)} = 0. \quad (4.9)$$

This means that a stationary effective action gives the physical values for the order parameters. Therefore, the effective action becomes a fundamental component of our theory for the analysis of phase transitions, as it incorporates fully the information of the BHH regardless of the phase of the system.

## 4.2 Physical quantities at finite temperature

Since we are describing the statistical state of a quantum system, it is convenient to establish the expected value of any arbitrary observable operator in the density matrix

formulation of quantum mechanics. As we are interested in finite temperature properties, the imaginary-time formalism should be of use. The expected value of an arbitrary operator  $\hat{A}(\tau)$  is given by

$$\langle \hat{A}(\tau) \rangle = \text{Tr} [\hat{\rho}_0 \hat{A}(\tau)], \quad (4.10)$$

where the operator  $\hat{\rho}_0$  is characterized by thermally distributed quantum states

$$\hat{\rho}_0 = \frac{e^{-\beta \hat{H}}}{Z}, \quad (4.11)$$

with  $Z = \text{Tr} [e^{-\beta \hat{H}}]$  being the partition function. In particular, when dealing with a quantum many-body system, the investigation of the Green's function plays an important role. All single-particle properties of such systems may be extracted from these functions. Accordingly, the Green's function can be defined as the thermal average of the time-ordered product of the bosonic creation and annihilation operators in the Heisenberg representation

$$G^{(n,m)}(\tau_1, i_1; \dots; \tau_n, i_n | \tau'_1, i'_1; \dots; \tau'_m, i'_m) = \frac{1}{Z} \text{Tr} \left\{ e^{-\beta \hat{H}} \hat{T} [\hat{a}_{i_1}(\tau_1) \dots \hat{a}_{i_n}(\tau_n) \hat{a}_{i'_1}^\dagger(\tau'_1) \dots \hat{a}_{i'_m}^\dagger(\tau'_m)] \right\}. \quad (4.12)$$

The expected value of physical quantities may be calculated out of these functions, which are also known as n-point correlation functions.

For the full BHH, an analytic form for the eigenstates and eigenenergies cannot be direct calculated, thus obtaining the exact expression for the Green's function is not possible in this case. With the use of the source term added to the Hamiltonian in the last section, we may approach such calculation approximately with a perturbative treatment. A series expansion of equation (4.3) gives

$$\hat{U}(\tau, \tau_0) = 1 - \int_{\tau_0}^{\tau} d\tau' \hat{H}(\tau') + \frac{1}{2} \int_{\tau_0}^{\tau} d\tau' \int_{\tau_0}^{\tau} d\tau'' \hat{T} [\hat{H}(\tau') \hat{H}(\tau'')] + \dots \quad (4.13)$$

The semi-group property of the imaginary-time evolution operator allows us to re-write it by isolating a subinterval from  $\tau - \Delta$  to  $\tau + \Delta$ , with  $\Delta > 0$ ,

$$\hat{U}(\beta, 0) = \hat{U}(\beta, \tau + \Delta) \hat{U}(\tau + \Delta, \tau - \Delta) \hat{U}(\tau - \Delta, 0). \quad (4.14)$$

With this expression, a functional derivative of the evolution operator with respect to the source  $j_i^*(\tau)$  gives

$$\frac{\delta \hat{U}(\beta, 0)}{\delta j_i^*(\tau)} = \hat{U}(\beta, \tau + \Delta) \frac{\delta \hat{U}(\tau + \Delta, \tau - \Delta)}{\delta j_i^*(\tau)} \hat{U}(\tau - \Delta, 0). \quad (4.15)$$

With the use of equation (4.13), we can obtain

$$\frac{\delta \hat{U}(\tau + \Delta, \tau - \Delta)}{\delta j_i^*(\tau)} = -\hat{a}_i + \int_{\tau - \Delta}^{\tau + \Delta} d\tau' [\Theta(\tau - \tau') \hat{a}_i \hat{H}(\tau') + \Theta(\tau' - \tau) \hat{H}(\tau') \hat{a}_i] - \dots, \quad (4.16)$$

where  $\Theta(\tau)$  is the Heaveside step function. In the limit of  $\Delta \rightarrow 0$  the equation (4.15) can be expressed as

$$\frac{\delta \hat{U}(\beta, 0)}{\delta j_i^*(\tau)} = -\hat{U}(\beta, \tau) \hat{a}_i \hat{U}(\tau, 0) = -\hat{U}(\beta, 0) \hat{a}_i(\tau), \quad (4.17)$$

with  $\hat{a}_i(\tau) = \hat{U}^{-1}(\tau, 0)\hat{a}_i\hat{U}(\tau, 0)$ . The Heisenberg operators are recovered by setting  $j_i(\tau) = j_i^*(\tau) = 0$ . Successive functional derivatives of (4.17) give us

$$\left. \frac{\delta^{(n+m)}\hat{U}(\beta, 0)}{\delta j_{i_1}^*(\tau_1)\dots\delta j_{i_n}^*(\tau_n)\delta j_{i'_1}(\tau'_1)\dots\delta j_{i'_m}(\tau'_m)} \right|_{j^*=j=0} = \hat{U}(\beta, 0)\hat{T}\left[\hat{a}_{i_1}(\tau_1)\dots\hat{a}_{i_n}(\tau_n)\hat{a}_{i'_1}^\dagger(\tau'_1)\dots\hat{a}_{i'_m}^\dagger(\tau'_m)\right]. \quad (4.18)$$

Finally, the trace of this equation leads to the Green's function in terms of the source-dependent partition function

$$G^{(n,m)}(\tau_1, i_1; \dots; \tau_n, i_n | \tau'_1, i'_1; \dots; \tau'_m, i'_m) = \frac{1}{Z[j^*, j]} \left. \frac{\delta^{(n+m)} Z[j^*, j]}{\delta j_{i_1}^*(\tau_1)\dots\delta j_{i_n}^*(\tau_n)\delta j_{i'_1}(\tau'_1)\dots\delta j_{i'_m}(\tau'_m)} \right|_{j^*=j=0}. \quad (4.19)$$

With this relation, physical quantities can be calculated from the partition function. Such function will also be obtained by means of a perturbative approach, on which we focus in the next section.

### 4.3 Perturbation theory

Since we cannot calculate the exact form of the eigenenergies and eigenstates of the full BHH analytically, we use perturbation theory as a tool to approximate the partition function of the system. With this purpose, we treat the BHH as the special case of a more general class of Hamiltonians which are composed by the sum of a local term plus a hopping term

$$\hat{H} = \hat{H}_l + \hat{H}_h, \quad (4.20)$$

with local and hopping term being defined respectively as

$$\hat{H}_l = \sum_i f_i(\hat{n}_i) \quad \text{and} \quad \hat{H}_h = - \sum_{ij} J_{ij} \hat{a}_i^\dagger \hat{a}_j. \quad (4.21)$$

The function  $f_i(\hat{n}_i)$  must include a dependency on the chemical potential as we are working in the grand canonical ensemble. The local term allows for the consideration of interactions between any finite number of bosons in the same lattice site and the hopping term accounts for the tunneling among sites arbitrarily distant. The BHH is recovered with the conditions

$$f_i(\hat{n}_i) = \frac{U}{2}\hat{n}_i(\hat{n}_i - 1) - \mu\hat{n}_i \quad \text{and} \quad J_{ij} = \begin{cases} J & \text{if } ij \text{ are nearest neighbors,} \\ 0 & \text{otherwise.} \end{cases} \quad (4.22)$$

We notice that the full Hamiltonian becomes local if the hopping term is neglected. For a deep lattice potential this parameter is small and the effect of the interaction between particles is strong. The hopping term can thus be used as an expansion parameter. We start by adding to the Hamiltonian the source term of equation (4.1)

$$\hat{H}(\tau) = \hat{H}_0(\tau) + \hat{H}_h, \quad (4.23)$$

where

$$\hat{H}_0(\tau) = \hat{H}_l + \hat{H}_s \quad , \quad \hat{H}_s = \sum_i \left[ j_i^*(\tau) \hat{a}_i + j_i(\tau) \hat{a}_i^\dagger \right]. \quad (4.24)$$

We can factorize the hopping-dependent part out of the imaginary-time evolution operator

$$\hat{U}(\tau, 0) = \hat{U}_0(\tau, 0) \hat{U}_h(\tau, 0), \quad (4.25)$$

where the unperturbed part  $\hat{U}_0(\tau, 0)$  obeys the following equation

$$-\frac{\partial \hat{U}_0(\tau, 0)}{\partial \tau} = \hat{H}_0(\tau) \hat{U}_0(\tau, 0), \quad (4.26)$$

with solution analogous to equation (4.3)

$$\hat{U}_0(\tau, \tau_0) = \hat{T} \left\{ \exp \left[ - \int_{\tau_0}^{\tau} d\tau' \hat{H}_0(\tau') \right] \right\}. \quad (4.27)$$

The interaction part of the evolution operator related to the hopping parameter can be constructed following equations (4.2) and (4.26), which gives

$$-\frac{\partial \hat{U}_h(\tau, 0)}{\partial \tau} = \hat{H}_h(\tau) \hat{U}_h(\tau, 0), \quad (4.28)$$

where we have  $\hat{H}_h(\tau) = \hat{U}_0^{-1}(\tau, 0) \hat{H}_s \hat{U}_0(\tau, 0)$ . The solution for the above equation can be put in a form similar to equation (4.3)

$$\hat{U}_h(\tau, \tau_0) = \hat{T} \left\{ \exp \left[ - \int_{\tau_0}^{\tau} d\tau' \hat{H}_h(\tau') \right] \right\}. \quad (4.29)$$

We can write the partition function as

$$Z[j^*, j] = \text{Tr} \left[ \hat{U}_0(\beta, 0) \hat{T} e^{-\int_0^\beta d\tau \hat{H}_h(\tau)} \right]. \quad (4.30)$$

With the use of equations (4.18) and (4.21) the partition function  $Z[j^*, j]$  can be written in terms of functional derivatives of the hopping-free partition function  $Z_0[j^*, j]$

$$Z[j^*, j] = \exp \left[ \sum_{ij} J_{ij} \int_0^\beta d\tau \frac{\delta^2}{\delta j_i^*(\tau) \delta j_j(\tau)} \right] Z_0[j^*, j], \quad (4.31)$$

where we have

$$Z_0[j^*, j] = \text{Tr} \left[ \hat{U}_0(\tau, 0) \right]. \quad (4.32)$$

The above expression shows that we can approximate the full partition function of the system by means of a hopping expansion. The hopping-free partition function is also calculated perturbatively in terms of the sources. Such powerful process of approximation can be thought of as a strong-coupling expansion [71]. A simple way to find the functionals of the theory is to use a diagrammatic notation, which we introduce in the next section.

## 4.4 Diagrammatic representation

The hopping-free partition function is calculated with  $J_{ij} = 0$ , thus it splits into a product of independent functions at each lattice site

$$Z_0[j^*, j] = \prod_i Z_{0i}[j^*, j]. \quad (4.33)$$

With the use of the imaginary-time evolution operator  $\hat{U}_0(\tau, 0)$ , such partition function can be written as

$$\begin{aligned} Z_{0i}[j^*, j] &= \text{Tr} \left[ e^{-\beta f_i(\hat{n}_i)} \hat{T} e^{-\int_0^\beta d\tau \hat{H}_s(\tau)} \right] \\ &= \text{Tr} \left[ e^{-\beta f_i(\hat{n}_i)} - \int_0^\beta d\tau \text{Tr} \left[ e^{-\beta f_i(\hat{n}_i)} \hat{H}_s(\tau) \right] + \dots \right] \end{aligned} \quad (4.34)$$

To simplify our diagrammatic representation, we define the functional

$$W[j^*, j] = \ln \{ Z[j^*, j] \} = -\beta F[j^*, j], \quad (4.35)$$

which can be expanded as a series of the sources  $j^*$  and  $j$  as

$$\begin{aligned} W[j^*, j] &= W^{(0)} + \sum_{ii'} \int_0^\beta d\tau \int_0^\beta d\tau' j_i^*(\tau) W_{ii'}^{(2)}(\tau; \tau') j_{i'}(\tau') \\ &+ \frac{1}{2!^2} \sum_{i_1 i_2 i'_1 i'_2} \int_0^\beta d\tau_1 \int_0^\beta d\tau_2 \int_0^\beta d\tau'_1 \int_0^\beta d\tau'_2 j_{i_1}^*(\tau_1) j_{i_2}^*(\tau_2) W_{i_1 i_2; i'_1 i'_2}^{(4)}(\tau_1, \tau_2; \tau'_1, \tau'_2) j_{i'_1}(\tau'_1) j_{i'_2}(\tau'_2) + \dots \end{aligned} \quad (4.36)$$

This functional is analogously separated in a sum of independent terms at each lattice site for the zero-hopping case

$$W_0[j^*, j] = \sum_i W_{0i}[j^*, j]. \quad (4.37)$$

We can expand each site dependent functional as a power series of sources  $j^*$  and  $j$

$$\begin{aligned} W_{0i}[j^*, j] &= W_{0i}^{(0)} + \int_0^\beta d\tau \int_0^\beta d\tau' j_i^*(\tau) W_{0i}^{(2)}(\tau; \tau') j_i(\tau') \\ &+ \frac{1}{2!^2} \int_0^\beta d\tau_1 \int_0^\beta d\tau_2 \int_0^\beta d\tau'_1 \int_0^\beta d\tau'_2 j_i^*(\tau_1) j_i^*(\tau_2) W_{0i}^{(4)}(\tau_1, \tau_2; \tau'_1, \tau'_2) j_i(\tau'_1) j_i(\tau'_2) + \dots \end{aligned} \quad (4.38)$$

This quantity is called the  $2n$ -point connected correlation function.

By using a notation similar to the one found in Ref. [72] for the Hubbard model, we can define the terms for the free functional  $W_0$  expansion diagrammatically as

$$W_{0i}^{(2n)}(\tau_1, \dots, \tau_n; \tau'_1, \dots, \tau'_n) = \begin{array}{c} \tau'_1 \\ \tau'_2 \\ \vdots \\ \tau'_n \end{array} \begin{array}{c} \longrightarrow \\ \longrightarrow \\ \longrightarrow \\ \longrightarrow \end{array} \begin{array}{c} \bullet \\ | \\ \bullet \end{array} \begin{array}{c} \longleftarrow \\ \longleftarrow \\ \longleftarrow \\ \longleftarrow \end{array} \begin{array}{c} \tau_1 \\ \tau_2 \\ \vdots \\ \tau_n \end{array}, \quad (4.39)$$

where each leg in the diagram corresponds to a time variable and the central point stands for a given lattice site. In this notation, the functional  $W_0[j^*, j]$  becomes the sum of 1-vertex



diagrams

$$W_0[j^*, j] = \bullet + \text{---}\bullet\text{---} + \frac{1}{2!^2} \text{---}\bullet\text{---} + \frac{1}{3!^2} \text{---}\bullet\text{---} + \dots \quad (4.40)$$

Each diagram in the above expression corresponds to a term of equation (4.38). To avoid confusion, we have shortened the notation by assuming that each unlabeled point means a sum over all lattice sites and each unlabeled inward (outward) line means a multiplication by  $j^*$  ( $j$ ) and integration from 0 to  $\beta$  in imaginary time. Each diagram presents a symmetry factor  $\left(\frac{1}{n_l}\right)^2$ , which corresponds to the number  $n_l$  of permutation between the inward and outward lines. These diagrams are called the connected diagrams.

With the definition of the energy functional  $W$ , the hopping-free partition function can be written as  $Z_0 = e^{W_0}$ . If we represent the  $l$ -th diagram by  $D_l$ , the unperturbed partition function becomes

$$Z_0 = e^{\sum_l D_l} = \prod_l e^{D_l} = \prod_l \sum_{n_l=0}^{\infty} \frac{1}{n_l!} D_l^{n_l}. \quad (4.41)$$

From this expression we see that  $Z_0$  is composed by products of diagrams multiplied by some symmetry factor. These are called the disconnected diagrams. Thus, we can express the unperturbed partition function diagrammatically as

$$Z_0[j^*, j] = e^{\bullet} \left[ \text{---}\bullet\text{---} + \frac{1}{2!} \text{---}\bullet\text{---} + \frac{1}{2!^2} \text{---}\bullet\text{---} + \frac{1}{2!^2} \text{---}\bullet\text{---} + \frac{1}{3!} \text{---}\bullet\text{---} + \frac{1}{3!^2} \text{---}\bullet\text{---} + \dots \right]. \quad (4.42)$$

The full partition function could be approximately obtained by applying the hopping expansion given by equation (4.31) to the above equation. Explicitly, the  $n$ -th order hopping approximation is given by the operator  $\frac{1}{n!} \sum_{ij} J_{ij} \int_0^\beta d\tau \frac{\delta^2}{\delta j_i^*(\tau) \delta j_j(\tau)}$  acting  $n$  times on  $Z_0[j^*, j]$ . The effect of the functional derivatives  $\frac{\delta}{\delta j_i^*(\tau)}$  and  $\frac{\delta}{\delta j_j(\tau)}$  on a local diagram is the introduction of an index  $i$  to its central vertex and the addition of a imaginary time variable  $\tau$  to its inward or outward lines, respectively. The result of the full operator acting on products of diagrams is to generate different diagrams by joining an inward open line of one diagram with the outward open line of another. Through this process, the first-order hopping correction to the partition function is given by

$$Z[j^*, j] = e^{\bullet} \left[ \text{---}\bullet\text{---} + \text{---}\bullet\text{---} + \frac{1}{2!} \text{---}\bullet\text{---} + \text{---}\bullet\text{---} + \frac{1}{2!} \text{---}\bullet\text{---} + \frac{1}{2!} \text{---}\bullet\text{---} + \frac{1}{2!^2} \text{---}\bullet\text{---} + \dots \right]. \quad (4.43)$$

This function is also called the generating functional of the full Green's functions. As a consequence of the so-called *linked cluster theorem* [73, 74], the logarithm of this function contains only connected diagrams. For this reason, the energy  $W[j^*, j]$  is called the generating functional of the connected diagrams or generating functional of the connected Green's functions.

Therefore, the energy functional  $W[j^*, j]$  is given by

$$W[j^*, j] = \bullet + \rightarrow \bullet \rightarrow + \rightarrow \bullet \bullet \rightarrow + \frac{1}{2!^2} \begin{array}{c} \nearrow \bullet \nwarrow \\ \searrow \bullet \swarrow \end{array} + \frac{1}{2!} \begin{array}{c} \nearrow \bullet \bullet \nwarrow \\ \searrow \bullet \swarrow \end{array} + \frac{1}{2!} \begin{array}{c} \nearrow \bullet \bullet \bullet \nwarrow \\ \searrow \bullet \swarrow \end{array} + \dots \quad (4.44)$$

In this work we focus on results of first-order hopping correction. We can now summarize the rules for calculating the generating functionals  $Z$  and  $W$  within the diagrammatic representation:

- The partition function can be obtained from the generator of connected diagrams by the relation  $Z = e^W$ ;
- The functional  $W$  is composed by a sum of connected diagrams each multiplied by a symmetry factor. Each connected diagram has a number  $n_v$  of vertices (points), a number  $n_l$  of external lines, divided into  $n_{j^*}$  inward and  $n_j$  outward lines, and a number  $n_i$  of internal lines between all vertices. We also define  $n_{v_i}$  as the number of vertex connected with lines;
- Our perturbation theory is based on two procedures: the expansion on the sources  $j_i^*(\tau)$  and  $j_i(\tau)$  and the hopping term expansion. The order of a diagram in the sources expansion is given by the number of inward and outward lines, whereas in the hopping expansion the order with respect to the hopping matrix  $J_{ij}$  is given by the number of internal lines connecting the vertices. In order to calculate the  $n$ -th order in the sources and the  $m$ -th order in the hopping matrix, we must sum all diagrams containing  $n$  external lines and  $m$  internal lines considering their symmetry factor;
- We calculate the symmetry factor by the following steps: First we take  $\frac{1}{n_i!}$ ; then we multiply it by  $\frac{1}{n_{v_i}!}$  for each kind of vertex in the diagram; for each vertex we multiply by  $\frac{1}{n_j!n_{j^*}!}$ ; and last multiply by the number of ways of joining the vertices so we obtain different diagrams.

The diagrammatic notation simplifies the calculation of our perturbative expansion. High-order terms can be obtained simply by following the above stated rules. We now turn our attention to the diagrammatic representation of the effective action, as it is the central element of our theory.

## 4.5 Effective action

In the last section, we have seen that the diagrammatic technique simplifies the calculation of the systems partition function by only considering the connected diagrams. This task could become even simpler with the introduction of the so-called *one-particle irreducible*



Applying a Legendre transformation to equation (4.36) we get the following form for the coefficients

$$\begin{aligned}
\Gamma^{(0)} &= W^{(0)} \\
\Gamma_{ii'}^{(2)}(\tau; \tau') &= [W^{(2)}]_{ii'}^{-1}(\tau; \tau') \\
\Gamma_{i_1 i_2; i'_1 i'_2}^{(4)}(\tau_1, \tau_2; \tau'_1, \tau'_2) &= \\
&\sum_{i''_1 i''_2 i''_1 i''_2} \int_0^\beta d\tau''_1 \int_0^\beta d\tau''_2 \int_0^\beta d\tau'''_1 \int_0^\beta d\tau'''_2 W_{i''_1 i''_2; i'_1 i'_2}^{(4)}(\tau_1, \tau_2; \tau''_1, \tau''_2) \\
&\times [W^{(2)}]_{i_1 i''_1}^{-1}(\tau_1; \tau''_1) [W^{(2)}]_{i_2 i''_2}^{-1}(\tau_2; \tau''_2) [W^{(2)}]_{i''_1 i'_1}^{-1}(\tau''_1; \tau'_1) [W^{(2)}]_{i''_2 i'_2}^{-1}(\tau''_2; \tau'_2).
\end{aligned} \tag{4.51}$$

The diagrams for the coefficients are

$$\begin{aligned}
\Gamma_{ii'}^{(2)}(\tau; \tau') &= i'; \tau' \text{ --- } \bigcirc \text{ --- } i; \tau, \\
\Gamma_{i_1 i_2; i'_1 i'_2}^{(4)}(\tau_1, \tau_2; \tau'_1, \tau'_2) &= \begin{array}{c} i'_2; \tau'_2 \text{ ---} \\ \text{---} \\ i'_1; \tau'_1 \text{ ---} \\ \text{---} \\ i_2; \tau_2 \text{ ---} \\ \text{---} \\ i_1; \tau_1 \text{ ---} \end{array} \bigcirc \begin{array}{c} i_2; \tau_2 \text{ ---} \\ \text{---} \\ i_1; \tau_1 \text{ ---} \end{array}.
\end{aligned} \tag{4.52}$$

Finally, the effective action in terms of the 1PI diagrams is

$$-\beta\Gamma[\psi^*, \psi] = \Gamma^{(0)} + \text{---} \bigcirc \text{---} + \frac{1}{2!^2} \begin{array}{c} \text{---} \\ \text{---} \\ \text{---} \\ \text{---} \end{array} \bigcirc \begin{array}{c} \text{---} \\ \text{---} \\ \text{---} \\ \text{---} \end{array} + \frac{1}{3!^2} \text{---} \bigcirc \text{---} + \dots \tag{4.53}$$

Explicit calculation of these diagrams allows us to investigate further details of phase transitions with a Landau theory. In the next section, we introduce a different representation with the aim of finding the mathematical expressions for such diagrams.

## 4.6 Matsubara frequencies

The imaginary time formulation of quantum statistical mechanics is also known as Matsubara formalism. In 1955, Takeo Matsubara proposed this approach by using an expansion of the ideal gas mean single-particle occupation number to define what today we call the Matsubara frequencies [76]. As the imaginary-time variable is defined over the interval from 0 to  $\beta$ , we can expand any single-variable function  $g(\tau)$  of our theory in a Fourier series such as

$$g(\tau) = \frac{1}{\beta} \sum_{\omega_l} e^{-i\omega_l \tau} g(\omega_l), \tag{4.54}$$

where the discrete variables  $\omega_l = \frac{2\pi l}{\beta}$  are the so-called Matsubara frequencies. The inverse transformation then becomes

$$g(\omega_l) = \int_0^\beta d\tau e^{i\omega_l \tau} g(\tau). \tag{4.55}$$

These transformations can also be defined for multi-variable functions such as the generating functionals  $W$  and  $\Gamma$ . With this transformation, equations (4.36) and (4.50) can be written as

$$\begin{aligned} W[j^*, j] &= W^{(0)} + \frac{1}{\beta^2} \sum_{ii'} \sum_{\omega\omega'} j_i^*(\omega) W_{ii'}^{(2)}(\omega, \omega') j_i(\omega') \\ &+ \frac{1}{2!^2} \frac{1}{\beta^4} \sum_{i_1 i_2 i'_1 i'_2} \sum_{\omega_1 \omega_2 \omega'_1 \omega'_2} j_{i_1}^*(\omega_1) j_{i_2}^*(\omega_2) W_{i_1 i_2 i'_1 i'_2}^{(4)}(\omega_1, \omega_2; \omega'_1, \omega'_2) j_{i'_1}(\omega'_1) j_{i'_2}(\omega'_2) + \dots, \end{aligned} \quad (4.56)$$

$$\begin{aligned} -\beta\Gamma[\psi^*, \psi] &= \Gamma^{(0)} + \frac{1}{\beta^2} \sum_{ii'} \sum_{\omega\omega'} \psi_i^*(\omega) \Gamma_{ii'}^{(2)}(\omega, \omega') \psi_i(\omega') \\ &+ \frac{1}{2!^2} \frac{1}{\beta^4} \sum_{i_1 i_2 i'_1 i'_2} \sum_{\omega_1 \omega_2 \omega'_1 \omega'_2} \psi_{i_1}^*(\omega_1) \psi_{i_2}^*(\omega_2) \Gamma_{i_1 i_2 i'_1 i'_2}^{(4)}(\omega_1, \omega_2; \omega'_1, \omega'_2) \psi_{i'_1}(\omega'_1) \psi_{i'_2}(\omega'_2) + \dots \end{aligned} \quad (4.57)$$

It turns out that working in the frequency space simplifies our calculations, as the systems that we are considering turn out to present time invariance. The diagrammatic expansion maintain the same form in Matsubara space. With this representation we can now compute the explicit form of the generating functionals.

## 4.7 Zeroth-hopping order result

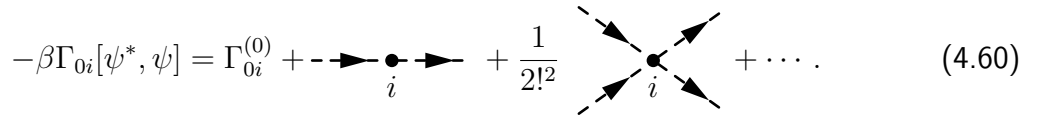
In order to find the expression for the effective action expansion coefficients, we start by considering the case where  $J_{ij} = 0$ . Similarly to the other generating functions of the theory, for the zero hopping case, the effective action can be separated into independent functions for each lattice site, thus giving

$$\Gamma_0[\psi^*, \psi] = \sum_i \Gamma_{0i}[\psi^*, \psi]. \quad (4.58)$$

The series representation for the zero-hopping local action  $\Gamma_{0i}$  is

$$\begin{aligned} -\beta\Gamma_{0i}[\psi^*, \psi] &= \Gamma_{0i}^{(0)} + \int_0^\beta d\tau \int_0^\beta d\tau' \psi_i^*(\tau) \Gamma_{0i}^{(2)}(\tau; \tau') \psi_i(\tau') \\ &+ \frac{1}{2!^2} \int_0^\beta d\tau_1 \int_0^\beta d\tau_2 \int_0^\beta d\tau'_1 \int_0^\beta d\tau'_2 \psi_i^*(\tau_1) \psi_i^*(\tau_2) \Gamma_{0i}^{(4)}(\tau_1, \tau_2; \tau'_1, \tau'_2) \psi_i(\tau'_1) \psi_i(\tau'_2) + \dots, \end{aligned} \quad (4.59)$$

or in the diagrammatic representation

$$-\beta\Gamma_{0i}[\psi^*, \psi] = \Gamma_{0i}^{(0)} + \text{---} \bullet_i \text{---} + \frac{1}{2!^2} \text{---} \bullet_i \text{---} + \dots \quad (4.60)$$


A Legendre transform of equation (4.38) gives for the zeroth-order term

$$\Gamma_{0i}^{(0)} = W_{0i}^{(0)} = \ln \sum_{n=0}^{\infty} e^{-\beta f_i(n)}. \quad (4.61)$$

The second-order term  $\Gamma_{0i}^{(2)}$  is given by the inverse of  $W_{0i}^{(2)}$ . As shown in Ref. [70], the full correlation functions can be decomposed into connected correlation functions. In our theory, this decomposition for the two-point function gives

$$G_{0i}^{(2)}(\tau, \tau') = W_{0i}^{(2)}(\tau, \tau') = \frac{1}{Z_{0i}} \text{Tr} \left\{ e^{-\beta \hat{H}_0} \hat{T} \left[ \hat{a}_i(\tau') \hat{a}_i^\dagger(\tau) \right] \right\}, \quad (4.62)$$

where a direct computation gives

$$W_{0i}^{(2)}(\tau, \tau') = \frac{1}{Z_{0i}^{(0)}} \sum_{n=0}^{\infty} e^{-\beta f_i(n)} \left[ \Theta(\tau - \tau') (n+1) e^{(\tau - \tau') [f_i(n) - f_i(n+1)]} \right. \\ \left. + \Theta(\tau' - \tau) n e^{(\tau' - \tau) [f_i(n) - f_i(n-1)]} \right]. \quad (4.63)$$

In the Matsubara representation, we get

$$W_{0i}^{(2)}(\omega, \omega') = \beta \delta_{\omega, \omega'} g_i(\omega), \quad (4.64)$$

where  $\delta_{\omega, \omega'}$  is the Kronecker delta and we have defined

$$g_i(\omega) = \frac{1}{Z_{0i}^{(0)}} \sum_{n=0}^{\infty} (n+1) \frac{e^{-\beta f_i(n+1)} - e^{-\beta f_i(n)}}{i\omega + f_i(n) + f_i(n+1)}, \quad (4.65)$$

where  $Z_{0i}^{(0)} = \sum_{n=0}^{\infty} e^{-\beta f_i(n)}$  is the first term in the hopping-free partition function expansion of equation (4.34).

The inverse of this function must obey the following conditions

$$\frac{1}{\beta} \sum_{\omega''} W_{0i}^{(2)}(\omega, \omega'') \Gamma_{0i}^{(2)}(\omega'', \omega') = \frac{1}{\beta} \sum_{\omega''} \Gamma_{0i}^{(2)}(\omega, \omega'') W_{0i}^{(2)}(\omega'', \omega') = -\beta \delta_{\omega, \omega'}, \quad (4.66)$$

thus giving

$$\Gamma_{0i}^{(2)}(\omega, \omega') = -\beta \delta_{\omega, \omega'} Z_{0i}^{(0)} \left[ \sum_{n=0}^{\infty} (n+1) \frac{e^{-\beta f_i(n+1)} - e^{-\beta f_i(n)}}{i\omega + f_i(n) + f_i(n+1)} \right]^{-1}. \quad (4.67)$$

In order to study phase transitions, we must also determine the term  $\Gamma_{0i}^{(4)}$ . The corresponding diagram is

$$\Gamma_{0i}^{(4)}(\omega_1, \omega_2; \omega'_1, \omega'_2) = \begin{array}{c} \omega'_2 \quad \omega_2 \\ \swarrow \quad \searrow \\ \bullet \quad \bullet \\ \downarrow \quad \downarrow \\ \bullet \quad \bullet \\ \swarrow \quad \searrow \\ \omega'_1 \quad \omega_1 \end{array} . \quad (4.68)$$

Similarly to equation (4.51), we can write

$$\Gamma_{0i}^{(4)}(\omega_1, \omega_2; \omega'_1, \omega'_2) = \frac{1}{\beta^4} \sum_{\omega''_1 \omega''_2 \omega'''_1 \omega'''_2} W_{0i}^{(4)}(\omega''_1, \omega''_2; \omega'''_1, \omega'''_2) \Gamma_{0i}^{(2)}(\omega_1, \omega''_1) \Gamma_{0i}^{(2)}(\omega_2, \omega''_2) \Gamma_{0i}^{(2)}(\omega'_1, \omega'''_1) \Gamma_{0i}^{(2)}(\omega'_2, \omega'''_2). \quad (4.69)$$

By using the decomposition of full correlation functions into the connected functions, we get

$$W_{0i}^{(4)}(\tau_1, \tau_2; \tau'_1, \tau'_2) = G_{0i}^{(4)}(\tau_1, \tau_2; \tau'_1, \tau'_2) - W_{0i}^{(2)}(\tau_1, \tau'_1)W_{0i}^{(2)}(\tau_2, \tau'_2) - W_{0i}^{(2)}(\tau_1, \tau'_2)W_{0i}^{(2)}(\tau_2, \tau'_1), \quad (4.70)$$

where explicitly, we have

$$\begin{aligned} G_{0i}^{(4)}(\tau_1, \tau_2; \tau'_1, \tau'_2) &= \frac{1}{Z_{0i}^{(0)}} \text{Tr} \left\{ e^{-\beta \hat{H}_0} \hat{T} \left[ \hat{a}_i(\tau_1) \hat{a}_i(\tau_2) \hat{a}_i^\dagger(\tau'_1) \hat{a}_i^\dagger(\tau'_2) \right] \right\} \\ &= \frac{1}{Z_{0i}^{(0)}} \sum_{n=0}^{\infty} e^{-\beta f_i(n)} \\ &\times \left[ \Theta(\tau_1 - \tau_2) \Theta(\tau_2 - \tau'_1) \Theta(\tau'_1 - \tau'_2) (n+1)(n+2) \right. \\ &\quad \times e^{\tau_1[f_i(n) - f_i(n+1)]} e^{\tau_2[f_i(n+1) - f_i(n+2)]} e^{\tau'_1[f_i(n+2) - f_i(n+1)]} e^{\tau'_2[f_i(n+1) - f_i(n)]} \\ &\quad + \Theta(\tau_1 - \tau'_1) \Theta(\tau_1 - \tau_2) \Theta(\tau_2 - \tau'_2) (n+1)^2 \\ &\quad \times e^{\tau_1[f_i(n) - f_i(n+1)]} e^{\tau'_1[f_i(n+1) - f_i(n)]} e^{\tau_2[f_i(n) - f_i(n+1)]} e^{\tau'_2[f_i(n+1) - f_i(n)]} \\ &\quad + \Theta(\tau'_1 - \tau_1) \Theta(\tau_1 - \tau_2) \Theta(\tau_2 - \tau'_2) n(n+1) \\ &\quad \times e^{\tau'_1[f_i(n) - f_i(n-1)]} e^{\tau_1[f_i(n-1) - f_i(n)]} e^{\tau_2[f_i(n) - f_i(n+1)]} e^{\tau'_2[f_i(n+1) - f_i(n)]} \\ &\quad + \Theta(\tau'_1 - \tau'_2) \Theta(\tau'_2 - \tau'_1) \Theta(\tau_1 - \tau_2) n(n-1) \\ &\quad \times e^{\tau'_1[f_i(n) - f_i(n-1)]} e^{\tau'_2[f_i(n-1) - f_i(n-2)]} e^{\tau_1[f_i(n-2) - f_i(n-1)]} e^{\tau_2[f_i(n-1) - f_i(n)]} \\ &\quad + \Theta(\tau'_1 - \tau_1) \Theta(\tau_1 - \tau'_2) \Theta(\tau'_2 - \tau_2) n^2 \\ &\quad \times e^{\tau'_1[f_i(n) - f_i(n-1)]} e^{\tau_1[f_i(n-1) - f_i(n)]} e^{\tau'_2[f_i(n) - f_i(n-1)]} e^{\tau_2[f_i(n-1) - f_i(n)]} \\ &\quad + \Theta(\tau_1 - \tau'_1) \Theta(\tau'_1 - \tau'_2) \Theta(\tau'_2 - \tau_2) n(n-1) \\ &\quad \times e^{\tau_1[f_i(n) - f_i(n+1)]} e^{\tau'_1[f_i(n+1) - f_i(n)]} e^{\tau'_2[f_i(n) - f_i(n-1)]} e^{\tau_2[f_i(n-1) - f_i(n)]} \\ &\quad \left. + \begin{array}{l} \tau_1 \leftrightarrow \tau_2 \\ \tau'_1 \leftrightarrow \tau'_2 \end{array} \right], \quad (4.71) \end{aligned}$$

where in the last line we indicate the extra terms with permutations of time variables  $\tau_1$  with  $\tau_2$  and  $\tau'_1$  with  $\tau'_2$ .

We must now compute  $G_{0i}^{(4)}$  in the Matsubara space. This calculation is very extensive as we must integrate each term in the above equation. To avoid such problem, we let the

explicit calculation in Appendix 1 and follow by only giving its result

$$\begin{aligned}
G_{0i}^{(4)}(\omega_1, \omega_2; \omega'_1, \omega'_2) = & \\
& \frac{\beta^2}{Z_{0i}^{(0)}} \left( \delta_{\omega_1 \omega'_1} \delta_{\omega_2 \omega'_2} + \delta_{\omega_1 \omega'_2} \delta_{\omega_2 \omega'_1} \right) \\
& \times \sum_{n=0}^{\infty} e^{-\beta f_i(n)} \left[ \frac{n+1}{f_i(n+1) - f_i(n) - i\omega_2} + \frac{n}{f_i(n-1) - f_i(n) + i\omega_2} \right] \\
& \quad \times \left[ \frac{n+1}{f_i(n+1) - f_i(n) - i\omega_1} + \frac{n}{f_i(n-1) - f_i(n) + i\omega_1} \right] \\
& + \frac{\beta}{Z_{0i}^{(0)}} \delta_{\omega'_1 + \omega'_2, \omega_1 + \omega_2} \sum_{n=0}^{\infty} e^{-\beta f_i(n)} \\
& \times \left[ \frac{(n+2)(n+1)}{[f_i(n+1) - f_i(n) - i\omega_2][f_i(n+2) - f_i(n) - i\omega'_1 - i\omega'_2][f_i(n+1) - f_i(n) - i\omega_1]} \right. \\
& \quad \left. + \frac{n(n-1)}{[f_i(n-1) - f_i(n) - i\omega_2][f_i(n-2) - f_i(n) - i\omega_1 - i\omega_2][f_i(n+1) - f_i(n) - i\omega'_1]} \right. \\
& - \left( \frac{n+1}{[f_i(n+1) - f_i(n) - i\omega_1][f_i(n+1) - f_i(n) - i\omega'_1]} \right. \\
& \quad \left. + \frac{n}{[f_i(n+1) - f_i(n) + i\omega_1][f_i(n+1) - f_i(n) + i\omega'_1]} \right) \\
& \times \left( \frac{n+1}{f_i(n+1) - f_i(n) - i\omega'_2} + \frac{n}{f_i(n-1) - f_i(n) + i\omega_2} \right) + \frac{\omega_1 \leftrightarrow \omega_2}{\omega'_1 \leftrightarrow \omega'_2} \Big].
\end{aligned} \tag{4.72}$$



With the use of equations (4.64), (4.65), and (4.70), we can write

$$\begin{aligned}
W_{0i}^{(4)}(\omega_1, \omega_2; \omega'_1, \omega'_2) = & \\
& \frac{\beta^2}{Z_{0i}^{(0)}} \left( \delta_{\omega_1 \omega'_1} \delta_{\omega_2 \omega'_2} + \delta_{\omega_1 \omega'_2} \delta_{\omega_2 \omega'_1} \right) \\
& \times \left[ \sum_{n=0}^{\infty} e^{-\beta f_i(n)} \left( \frac{n+1}{f_i(n+1) - f_i(n) - i\omega_2} + \frac{n}{f_i(n-1) - f_i(n) + i\omega_2} \right) \right. \\
& \quad \times \left( \frac{n+1}{f_i(n+1) - f_i(n) - i\omega_1} + \frac{n}{f_i(n-1) - f_i(n) + i\omega_1} \right) \\
& \quad - \frac{1}{Z_{0i}^{(0)}} \sum_{n,m=0}^{\infty} e^{-\beta[f_i(n)+f_i(m)]} \left( \frac{n+1}{f_i(n+1) - f_i(n) - i\omega_2} + \frac{n}{f_i(n-1) - f_i(n) + i\omega_2} \right) \\
& \quad \left. \times \left( \frac{m+1}{f_i(m+1) - f_i(m) - i\omega_1} + \frac{m}{f_i(m-1) - f_i(m) + i\omega_1} \right) \right] \\
& + \frac{\beta}{Z_{0i}^{(0)}} \delta_{\omega'_1 + \omega'_2, \omega_1 + \omega_2} \sum_{n=0}^{\infty} e^{-\beta f_i(n)} \\
& \quad \times \left[ \frac{(n+2)(n+1)}{[f_i(n+1) - f_i(n) - i\omega'_2][f_i(n+2) - f_i(n) - i\omega'_1 - i\omega'_2][f_i(n+1) - f_i(n) - i\omega_1]} \right. \\
& \quad + \frac{n(n-1)}{[f_i(n-1) - f_i(n) + i\omega_2][f_i(n-2) - f_i(n) + i\omega_1 + i\omega_2][f_i(n-1) - f_i(n) - i\omega'_1]} \\
& \quad - \left( \frac{n+1}{[f_i(n+1) - f_i(n) - i\omega_1][f_i(n+1) - f_i(n) - i\omega'_1]} \right. \\
& \quad \left. + \frac{n}{[f_i(n+1) - f_i(n) + i\omega_1][f_i(n+1) - f_i(n) + i\omega'_1]} \right) \\
& \quad \left. \times \left( \frac{n+1}{f_i(n+1) - f_i(n) - i\omega'_2} + \frac{n}{f_i(n-1) - f_i(n) + i\omega_2} \right) + \frac{\omega_1 \leftrightarrow \omega_2}{\omega'_1 \leftrightarrow \omega'_2} \right]. \tag{4.73}
\end{aligned}$$

By using the above equation together with equations (4.64) and (4.69), we can find

$$\Gamma_{0i}^{(4)}(\omega_1, \omega_2; \omega'_1, \omega'_2) = \frac{W_{0i}^{(4)}(\omega_1, \omega_2; \omega'_1, \omega'_2)}{g(\omega_1)g(\omega'_1)g(\omega_2)g(\omega'_2)}. \tag{4.74}$$

In the zero temperature limit, equations (4.61), (4.65) and (4.73) become respectively

$$\frac{1}{\beta} \Gamma_{0i}^{(0)} \rightarrow f_i(n), \tag{4.75}$$

$$g_i(\omega) \rightarrow \frac{n}{f_i(n-1) - f_i(n) + i\omega} + \frac{n+1}{f_i(n) - f_i(n+1) + i\omega}, \tag{4.76}$$

$$\begin{aligned}
W_{0i}^{(4)}(\omega_1, \omega_2; \omega'_1, \omega'_2) \rightarrow & \\
& 2\pi\delta(\omega'_1 + \omega'_2 - \omega_1 - \omega_2) \\
& \times \left[ \frac{(n+2)(n+1)}{[f_i(n+1) - f_i(n) - i\omega'_2][f_i(n+2) - f_i(n) - i\omega'_1 - i\omega'_2][f_i(n+1) - f_i(n) - i\omega_1]} \right. \\
& + \frac{n(n-1)}{[f_i(n-1) - f_i(n) + i\omega_2][f_i(n-2) - f_i(n) + i\omega_1 + i\omega_2][f_i(n-1) - f_i(n) - i\omega'_1]} \\
& - \left( \frac{n+1}{[f_i(n+1) - f_i(n) - i\omega_1][f_i(n+1) - f_i(n) - i\omega'_1]} \right. \\
& \quad \left. + \frac{n}{[f_i(n+1) - f_i(n) + i\omega_1][f_i(n+1) - f_i(n) + i\omega'_1]} \right) \\
& \left. \times \left( \frac{n+1}{f_i(n+1) - f_i(n) - i\omega'_2} + \frac{n}{f_i(n-1) - f_i(n) + i\omega_2} \right) + \frac{\omega_1 \leftrightarrow \omega_2}{\omega'_1 \leftrightarrow \omega'_2} \right], \tag{4.77}
\end{aligned}$$

where we have used the following transformation for the Matsubara frequency sums and the Kronecker delta symbol

$$\frac{1}{\beta} \sum_{\omega} \rightarrow \frac{1}{2\pi} \int d\omega \quad \text{and} \quad \beta\delta_{\omega, \omega'} \rightarrow 2\pi\delta(\omega - \omega'). \tag{4.78}$$

We now have all information needed for our Landau theory for the effective action. We proceed by computing the first-order hopping correction for such functional.

## 4.8 First-hopping order result

Within our diagrammatic representation, we can observe that the only 1PI function which presents first-order hopping contribution is the two-point function  $W_{ii'}^{(1PI)}(\tau; \tau')$ . Hence, the only term in the effective action expansion which gets first-order hopping approximations is  $\Gamma^{(2)}$ . Diagrammatically, the full two-point function with first-order hopping correction is given by

$$W_{ii'}(\omega; \omega') \approx \delta_{ii'} \begin{array}{c} \text{---} \bullet \text{---} \bullet \text{---} \bullet \text{---} \\ \omega' \quad i \quad \omega \quad \omega' \quad i' \quad i \quad \omega \end{array}, \tag{4.79}$$

As we have seen from equations (4.51), by perturbatively inverting this expression, we get

$$\Gamma_{ij}^{(2)}(\omega, \omega') \approx \delta_{ij} \begin{array}{c} \text{---} \bullet \text{---} \\ \omega' \quad i \quad \omega \end{array} + \beta\delta_{\omega, \omega'} J_{ij}. \tag{4.80}$$

The zeroth-hopping order result (4.67) allows us to rewrite the above equation as

$$\Gamma_{ij}^{(2)}(\omega, \omega') \approx \beta\delta_{\omega, \omega'} J_{ij} - \beta\delta_{\omega, \omega'} \delta_{ij} Z_{0i}^{(0)} \left[ \sum_{n=0}^{\infty} (n+1) \frac{e^{-\beta f_i(n+1)} - e^{-\beta f_i(n)}}{i\omega + f_i(n) + f_i(n+1)} \right]^{-1}. \tag{4.81}$$

Thus, up to first order the effective action assumes the form

$$\Gamma[\psi^*, \psi] \approx \Gamma_0[\psi^*, \psi] - \frac{1}{\beta^2} \sum_{\omega} \sum_{ij} J_{ij} \psi_i^*(\omega) \psi_i(\omega) + \mathcal{O}(|\psi|^4). \quad (4.82)$$

It turns out that the first-hopping order correction for the effective action is already sufficient to improve the results obtained by mean field theory [41, 42]. Therefore, in the next chapter, we use this approximation to investigate phase transitions in the Bose-Hubbard model in the presence of on-site disorder.

## 5 Disordered Bose-Hubbard model

The interplay between disorder localization effects and superfluidity is studied in this chapter. In particular, we apply our field theoretical effective-action approach to determine the phase boundary for the phase transition from the superfluid to insulating phases presented by the disordered Bose-Hubbard model. By considering the case of static diagonal disorder, we introduce a disorder ensemble average and define a homogeneous order parameter. Uniform and Gaussian disorder distributions are considered. A comparison between the results for the superfluid density of mean-field theory and effective-action method is made. Furthermore, we propose the introduction of new order parameters in order to obtain detailed information about the Bose-glass phase.

### 5.1 Disorder ensemble average

Disorder in the BHH is usually addressed through the introduction of a local chemical potential  $\mu \rightarrow \mu + \epsilon_i$ ,

$$\hat{H}_{BH} = \frac{U}{2} \sum_i \hat{n}_i(\hat{n}_i - 1) - \sum_i (\mu + \epsilon_i) \hat{n}_i - J \sum_{\langle ij \rangle} \hat{a}_i^\dagger \hat{a}_j. \quad (5.1)$$

Such consideration is often referred to as diagonal disorder. The derivation of such equation follows the same path shown in chapter 2 with the separation of the external potential into an optical lattice part and a trapping part  $V_{trap}(\mathbf{r})$  [25]. With this consideration one can obtain

$$\epsilon_i = \int d^3\mathbf{r} V_{trap}(\mathbf{r}) |w(\mathbf{r} - \mathbf{r}_i)|^2 \approx V_{trap}(\mathbf{r}_i), \quad (5.2)$$

where the approximation is based on the assumption that  $V_{trap}(\mathbf{r})$  varies slowly and its characteristic length is much larger than the spatial extent of the Wannier function  $w(\mathbf{r} - \mathbf{r}_i)$ . Thus, in practice,  $\epsilon_i$  represents a local imperfection in the periodic lattice potential caused by the trapping potential. Disorder is achieved by letting such parameter vary randomly, which means that the chemical potential assumes values according to some probability distribution at each site.

In order to deal with the problem of a random chemical potential, we assume its time scale to be greater when compared to the thermodynamic time scale. In this way the chemical potential can be considered to be frozen in time. In addition, the magnitude of  $\epsilon_i$  at each lattice site can be regarded as spatially uncorrelated thus varying within a range where each value appears with a specific probability [77, 78]. In this fashion, such parameter satisfies a probability distribution  $p(\epsilon_i)$  of some kind, such as an uniform or a Gaussian distribution. Consequently, it becomes necessary to define, along with the quantum mechanical average of

equation (4.10), a disorder ensemble average. For an arbitrary quantity  $A_i$  we can express such average as

$$\overline{A_i} = \prod_i \int d\epsilon_i A_i p(\epsilon_i). \quad (5.3)$$

The disorder ensemble average can be used to define a different order parameter, which we intend to do in the next section. The disorder-averaged effective action can be found as an expansion in this new order parameter in a similar manner as before. We can use such functional to study quantum phase transition in the Bose-Hubbard Model with on-site disorder.

## 5.2 Static properties

In its equilibrium state, the BHH preserves spatial and temporal symmetry. Hence, when computing equilibrium properties it is sufficient to assume homogeneity. Due to the presence of a local chemical potential in the disordered model, such assumption is not valid for the space variable. However, we can use the disorder ensemble average to define a new order parameter

$$\overline{\psi_i(\tau)} = \overline{\langle \hat{a}_i(\tau) \rangle} = \psi_{eq}, \quad (5.4)$$

which is homogeneous and can be used to calculate the effective action. In the Matsubara representation such parameter becomes

$$\overline{\psi_i(\omega)} = \beta \delta_{\omega,0} \psi_{eq}. \quad (5.5)$$

In order to obtain the disordered effective action, we first compute the disorder-averaged free-energy functional  $\overline{W}$ . In Matsubara space such quantity is given by

$$\begin{aligned} \overline{W}[j^*, j] &= \overline{W^{(0)}} + \frac{1}{\beta^2} \sum_{ii'} \sum_{\omega\omega'} j_i^*(\omega) \overline{W_{ii'}^{(2)}}(\omega, \omega') j_i(\omega') \\ &+ \frac{1}{2!^2} \frac{1}{\beta^4} \sum_{i_1 i_2 i'_1 i'_2} \sum_{\omega_1 \omega_2 \omega'_1 \omega'_2} j_{i_1}^*(\omega_1) j_{i_2}^*(\omega_2) \overline{W_{i_1 i_2 i'_1 i'_2}^{(4)}}(\omega_1, \omega_2; \omega'_1, \omega'_2) j_{i'_1}(\omega'_1) j_{i'_2}(\omega'_2) + \dots \end{aligned} \quad (5.6)$$

Using equation (5.5), a Legendre transformation of the above expression in first-order hopping expansion gives

$$\overline{\Gamma^{(0)}} = \overline{W^{(0)}} = \frac{1}{\beta} \prod_i \int \left[ \ln \sum_{n=0}^{\infty} e^{-\beta f_i(n)} \right] p(\epsilon_i) d\epsilon_i, \quad (5.7)$$

$$\overline{\Gamma_{ij}^{(2)}}(0, 0) \approx \beta J_{ij} - \beta \delta_{ij} \frac{1}{\overline{g_i}(0)}, \quad (5.8)$$

$$\overline{\Gamma_{0i}^{(4)}}(0, 0; 0, 0) = \frac{\overline{W_{0i}^{(4)}}(0, 0; 0, 0)}{\overline{g_i}(0) \overline{g_i}(0) \overline{g_i}(0) \overline{g_i}(0)}, \quad (5.9)$$

where  $\overline{g_i}(0)$  and  $\overline{W_{0i}^{(4)}}(0, 0; 0, 0)$  are obtained by making  $\omega = 0$  and then taking the disorder ensemble average of equations (4.65) and (4.73).

Analogously to Ref. [40–42], we make use of the so-called effective potential, which consists of the effective action per lattice site. In the disordered case such quantity becomes

$$\bar{\Gamma}_{pot} = \frac{\bar{\Gamma}}{N_s}. \quad (5.10)$$

With the use of equation (5.5), the Landau expansion of the effective potential becomes

$$\bar{\Gamma}_{pot} = \bar{a}_0 + \bar{a}_2|\psi|^2 + \bar{a}_4|\psi|^4 + \dots, \quad (5.11)$$

with coefficients given by

$$\bar{a}_0 = \overline{\Gamma^{(0)}}, \quad (5.12)$$

$$\bar{a}_2 = \frac{\overline{\Gamma_{ij}^{(2)}}(0, 0)}{\beta N_s}, \quad (5.13)$$

$$\bar{a}_4 = \frac{\overline{\Gamma_{0i}^{(4)}}(0, 0; 0, 0)}{2!^2 \beta N_s}. \quad (5.14)$$

These coefficients can be explicitly obtained with the use of equations (4.65), (4.73), and (4.81). We have now all information we needed to the analysis of the superfluid-insulator transition. With the choice for a specific probability distribution for the local chemical potential, we can investigate further the effect of disorder in the phase boundary.

### 5.3 Boundary between superfluid and non-superfluid phases

Following the theory discussed in Chapter 3, we must start our analysis of the superfluid to non-sperfluid phase transition by verifying if  $a_4$  is positive. We use equations (4.65), (4.73), (4.74), and (5.14) to calculate it exactly. As we can see in Fig. (13), we have always  $a_4 \geq 0$  for zero and finite temperatures.

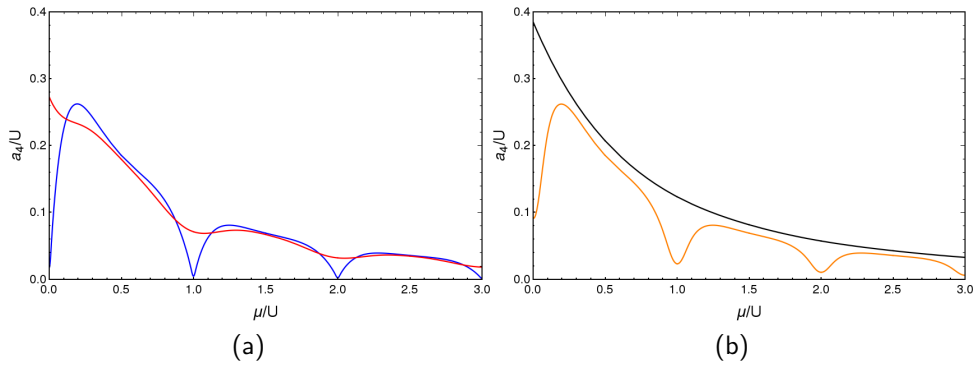


Figure 13 – Coefficient  $a_4$  at different temperatures. The blue and red lines in image (a) and the orange and black lines in image (b) correspond respectively to the temperatures  $\beta \rightarrow \infty$ ,  $\beta = 10/U$ ,  $\beta = 50/U$ , and  $\beta = 3/U$ .

As the disorder average is based on the integration of such coefficient,  $\overline{a_4}$  is also always positive. Such result allows us to determine the phase of the system by only evaluating the sign of  $\overline{a_2}$ . Thus, the phase boundary corresponds to the condition that  $\overline{a_2} = 0$ . In first-order hopping approximation, by making equation (5.13) equal to zero we get

$$Jz = \frac{1}{g_i(0)}, \quad (5.15)$$

these equation explicitly reads

$$\frac{1}{Jz} = \int d\epsilon_i \frac{p(\epsilon_i)}{Z_{0i}^{(0)}} \left[ \sum_{n=0}^{\infty} (n+1) \frac{e^{-\beta f_i(n+1)} - e^{-\beta f_i(n)}}{f_i(n) + f_i(n+1)} \right], \quad (5.16)$$

where we have

$$Z_{0i}^{(0)} = \sum_{n=0}^{\infty} e^{-\beta f_i(n)} \quad \text{and} \quad f_i(n) = \frac{U}{2} n(n-1) - (\mu + \epsilon_i)n. \quad (5.17)$$

We can now proceed by considering different probability distributions and investigate its influence in the phase boundary.

### 5.3.1 Pure case

The pure case is obtained if we consider that the probability distribution is localized in a definite value, i.e.,  $p(\epsilon) = \delta(\epsilon)$ . From equation (5.16) we get

$$\frac{1}{Jz} = \frac{1}{Z_0^{(0)}} \left[ \sum_{n=0}^{\infty} (n+1) \frac{e^{-\beta f(n+1)} - e^{-\beta f(n)}}{f(n) + f(n+1)} \right], \quad (5.18)$$

where  $Z_0^{(0)}$  and  $f(n)$  were found by setting  $\epsilon_i = 0$  in equation (5.17).

These result was already shown in Ref. [42]. In the zero temperature limit, such result becomes equal to the expression of equation (3.17), which is the phase boundary prediction of mean-field theory. Therefore, for the pure case, the first-hopping order for the effective action gives the same result as second order mean-field approximation for the phase boundary. However, this fact does not imply an equivalence between the two methods. As we have already stated, the mean-field theory predicts non-physical results such as decreasing condensate/superfluid density for strong hopping and negative compressibility in the region far from the boundary, while the effective-action approach presents an consistently increasing condensate density and always positive compressibility, as shown in Ref. [41].

### 5.3.2 Uniform homogeneous disorder distribution

We now move on to consider an homogeneous uniform disorder probability distribution such as

$$p(\epsilon_i) = \frac{1}{\Delta} \left[ \Theta \left( \epsilon_i + \frac{\Delta}{2} \right) - \Theta \left( \epsilon_i - \frac{\Delta}{2} \right) \right], \quad (5.19)$$

with each  $\epsilon_i$  restricted to the interval  $[-\frac{\Delta}{2}, \frac{\Delta}{2}]$ , where the value of  $\Delta$  determines the length of the interval. For such disorder distribution equation (5.16) becomes

$$\frac{1}{Jz} = \frac{1}{\Delta} \int_{\epsilon_i - \frac{\Delta}{2}}^{\epsilon_i + \frac{\Delta}{2}} \frac{d\epsilon_i}{Z_{0i}^{(0)}} \left[ \sum_{n=0}^{\infty} (n+1) \frac{e^{-\beta f_i(n+1)} - e^{-\beta f_i(n)}}{f_i(n) + f_i(n+1)} \right]. \quad (5.20)$$

In order to analyze the above integral, we first consider the zero temperature limit assuming also the  $\mu$  is restricted to the interval  $[U(n-1), Un]$ , with  $n$  being a positive integer. In such case, the result is given by

$$\frac{1}{Jz} = \frac{1}{\Delta} \left[ n \ln \left( \frac{\mu - U(n-1) + \frac{\Delta}{2}}{\mu - U(n-1) - \frac{\Delta}{2}} \right) - (n+1) \ln \left( \frac{Un - \mu - \frac{\Delta}{2}}{Un - \mu + \frac{\Delta}{2}} \right) \right], \quad (5.21)$$

if  $\mu \in [U(n-1) - \frac{\Delta}{2}, Un - \frac{\Delta}{2}]$ , and  $Jz = 0$  otherwise. This result is exactly the same as the one encountered by K. V. Krutitsky, A. Pelster, and R. Graham in Ref. [38], where they used the same mean-field approach following Ref. [79]. Also, if we take the limit  $\Delta \rightarrow 0$ , the result of the mean-field phase boundary of equation (3.17) is recovered. The finite and zero-temperature results are plotted in Fig. (14).

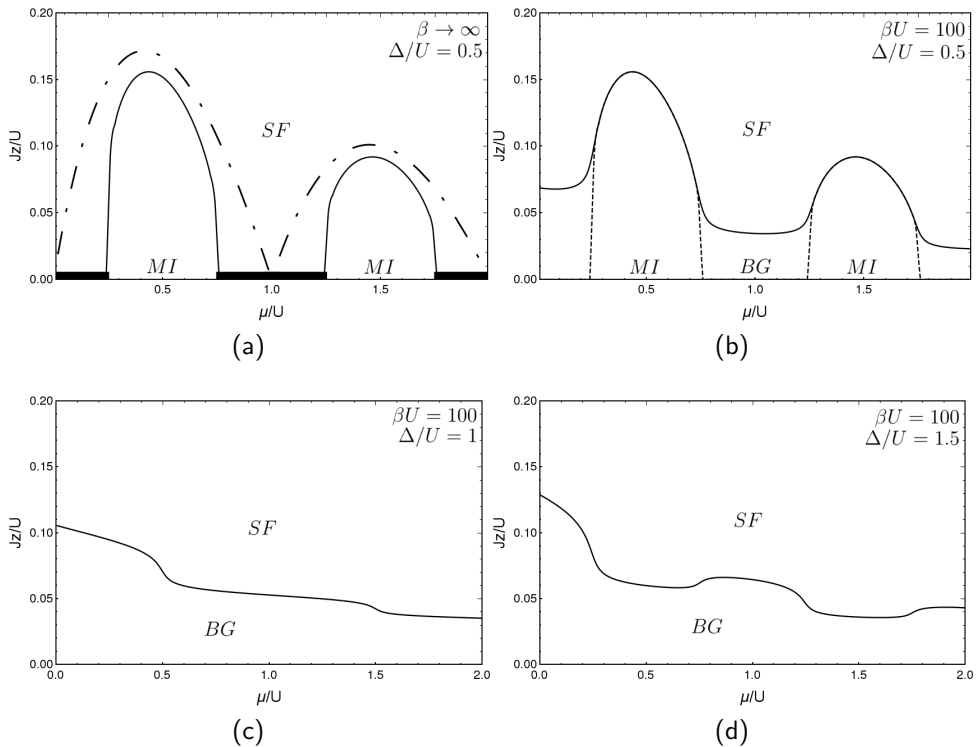


Figure 14 – Phase Boundary for homogeneous disorder distribution. Figure (a) shows the zero temperature limit, where the Bose-Glass phase exists only for  $J = 0$ , which corresponds to the thick black lines. The dash-dotted line indicates the pure case boundary of equation (3.17). In figure (b) we see the finite temperature solution, where a Bose-glass exists for  $J \neq 0$  as well. The dashed line represents the zero temperature solution. In figure (c) and (d) disorder becomes too strong and the Mott-Insulator phase disappears. *MI*, *BG*, and *SF* represent the Mott-insulator, Bose-glass, and superfluid phases respectively.



The phase boundary at the zero-temperature limit (figure (a)) shows a Mott lobe structure, where the size of the lobes decreases for an increasing disorder parameter  $\Delta$ . Such parameter limits the interval of integration where the Bose glass can exist. In the case of  $\Delta < U$ , for zero temperature the Bose glass region is suppressed to the case of vanishing hopping parameter. However, for finite temperature, such phase emerges between the Mott lobes. The phase boundary goes upwards and the size of the non-superfluid region expands. In comparison with the pure case, where a notable shift in the Mott insulator-superfluid boundary is only achieved for temperatures of the order of  $\frac{1}{\beta U} = \frac{k_B T}{U} \sim 1$  [80], for the case of homogeneous disorder a small increase in temperature, i.e.  $\frac{1}{\beta U} = \frac{k_B T}{U} = 0.01$ , changes rather significantly the phase boundary. For  $\Delta \geq U$ , the zero temperature transition line is restricted to  $J = 0$  for any value of  $\mu$ , thus the Mott lobes are suppressed and the superfluid phase dominates for positive magnitudes of the hopping parameter. In the finite temperature case of figures (c) and (d), the Bose-glass phase dominates the non-superfluid region as the Mott insulator cease to exist.

### 5.3.3 Gaussian disorder distribution

A more realistic treatment to the randomness of the local chemical potential would be accomplished by considering a Gaussian probability distribution,

$$p(\epsilon_i) = \frac{1}{\Delta\sqrt{2\pi}} \exp\left\{-\frac{\epsilon_i^2}{2\Delta^2}\right\}, \quad (5.22)$$

where, for such distribution,  $\Delta$  assumes the role of a standard deviation, that is it quantifies the dispersion around the set of possible values for the random variable. The integral of equation (5.16) would be carried out through all the domain of possible values of  $\epsilon_i$ , i.e.,

$$\frac{1}{Jz} = \frac{1}{\Delta\sqrt{2\pi}} \int_{-\infty}^{\infty} \frac{d\epsilon_i}{Z_{0i}^{(0)}} \left[ \sum_{n=0}^{\infty} (n+1) \frac{e^{-\beta f_i(n+1)} - e^{-\beta f_i(n)}}{f_i(n) + f_i(n+1)} \right] \exp\left\{-\frac{\epsilon_i^2}{2\Delta^2}\right\}. \quad (5.23)$$

The finite temperature solution to these integral gives us the phase boundary shown in Fig. (15).

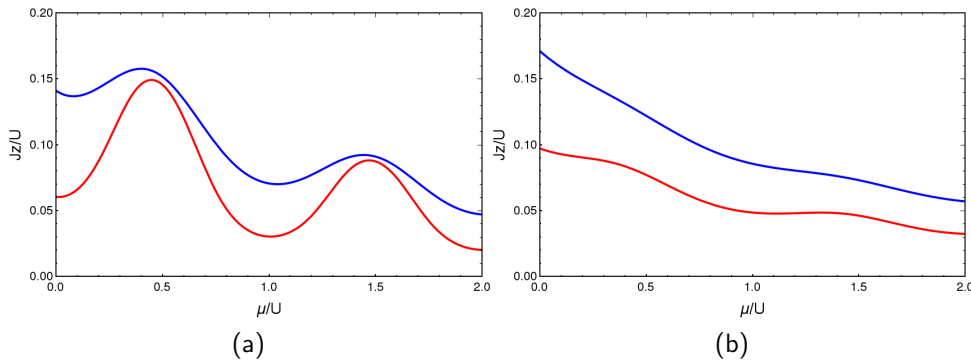


Figure 15 – Finite temperature phase boundary for a Gaussian disorder distribution. The curves red and blue indicate the temperatures  $\beta U = 100$  and  $\beta U = 15$ , respectively. In (a) we have  $\Delta/U = 0.15$  and in (b) we have  $\Delta/U = 0.35$ .

Since the Gaussian disorder distribution extends to the entire interval  $]-\infty, \infty[$  even in the weak disorder case, no Mott-insulating phase can occur and the whole region below the phase boundaries shown in Fig. (15) corresponds to the Bose-glass phase. Above such phase boundaries we have the superfluid phase. We can see, analogously to the result obtained for the homogeneous disorder distribution, that an increase in temperature makes the phase boundary to go upwards. Image (a) shows local minima around integer chemical potential  $\mu/U$  for the transition line. In the case of stronger disorder in image (b) such local minima almost disappear and the phase boundary becomes smooth.

In the present work we do not calculate the zero-temperature phase boundary. Instead, we give an intuition of how such calculation could be carried out. By using the zero temperature limit of  $g_i(\omega)$  given by equation (4.76), one can calculate the disorder ensemble average by means of principal value integration around some critical chemical potential. The specific disorder distribution does not affect the result of such computation. In this way, the zero temperature phase boundary could be obtained.

## 5.4 Superfluid density

We can use our effective-action method to calculate the superfluid density. As we have already stated in Chapter 3, such quantity is defined as the part of the systems density that remains at rest when the system receives a constant velocity boost. For the effective action, the phase factor presented in equation (3.21) for the mean-field superfluid density calculation is translated as

$$\psi_j(\tau) \rightarrow \psi_j e^{-ir_j \cdot \phi/L}. \quad (5.24)$$

If we describe the kinetic energy of the superfluid in terms of the difference  $\Gamma(\phi) - \Gamma(\mathbf{0})$ , the superfluid density can be defined as

$$\rho_s = \lim_{\phi \rightarrow 0} \frac{2L^2}{N_s J d^2 \phi^2} [\Gamma(\phi) - \Gamma(\mathbf{0})], \quad (5.25)$$

where  $\Gamma(\phi)$  represents the effective action transformed by the phase  $\phi$ .

We consider first-hopping order approximation and use the disorder-averaged Matsubara order parameter of equation (5.5). Using the transformation (5.24) into equation (5.25) we can write

$$\rho_s = \lim_{\phi \rightarrow 0} \frac{2L^2}{N_s J d^2 \phi^2} |\psi_{eq}|^2 \sum_{ij} J_{ij} [1 - e^{-i(\mathbf{r}_i - \mathbf{r}_j) \cdot \phi/L}]. \quad (5.26)$$

Considering hopping only over nearest neighbors and choosing the direction of  $\phi$  along one of the lattice vectors, the above equation becomes

$$\rho_s = \lim_{\phi \rightarrow 0} \frac{L^2}{d^2 \phi^2} |\psi_{eq}|^2 [2 - 2 \cos(d\phi/L)] = |\psi_{eq}|^2. \quad (5.27)$$

Thus, in first-hopping order approximation the superfluid and condensate density coincide, just as the result we had for mean-field theory. However, by using the expression

$$|\psi|^2 = -\frac{\overline{a_2}}{2\overline{a_4}}, \quad (5.28)$$

we can compare the disorder result for both approaches in the zero temperature case. Such comparison is shown in Fig. (16) for both Gaussian and uniform disorder distributions.

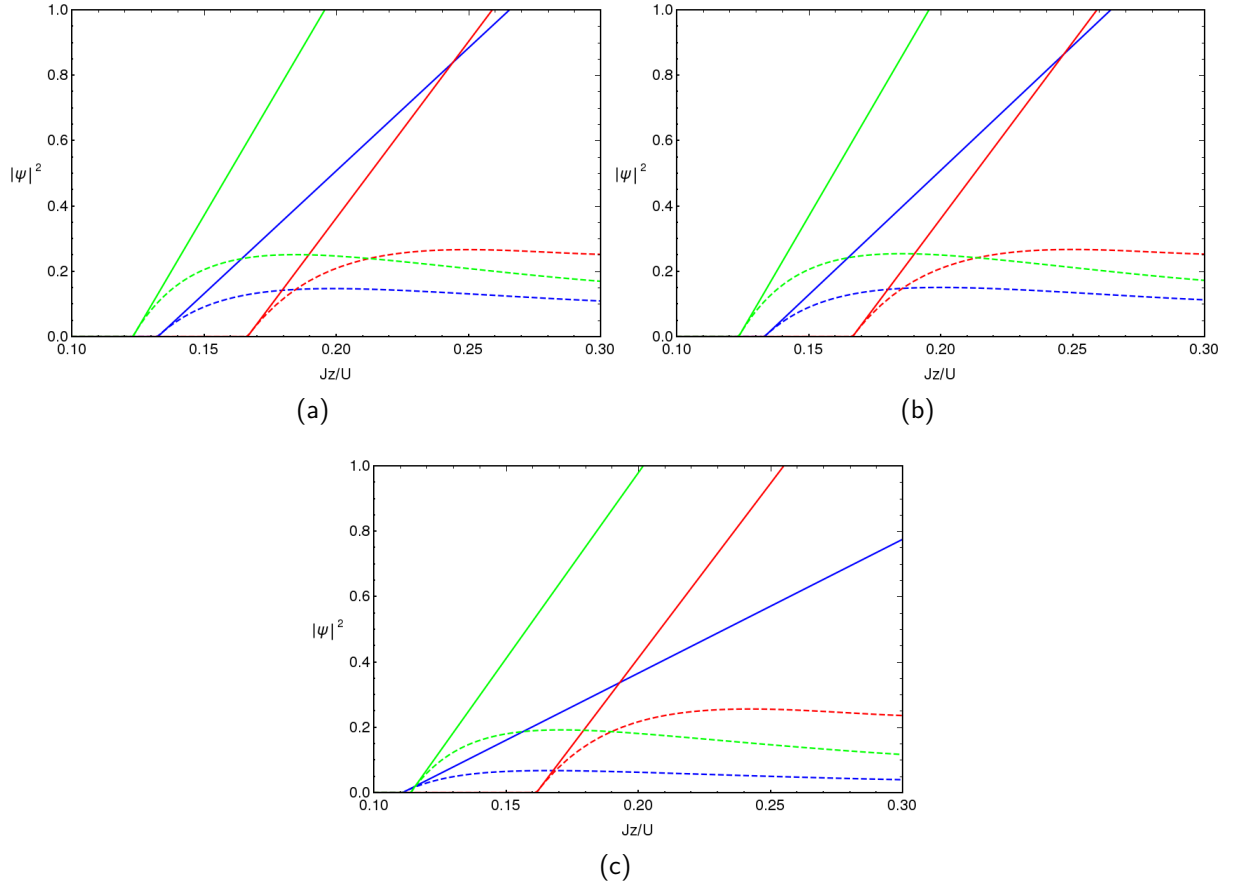


Figure 16 – Condensate/superfluid density as a function of the hopping parameter for Gaussian disorder distribution. The blue, red, and green lines correspond to  $\mu/U = 0.2$ ,  $\mu/U = 0.5$ , and  $\mu/U = 0.7$ , respectively. The dashed lines indicates the mean-field theory solution, while the continuous lines represent the effective-action method. Images (a) and (b) correspond respectively to Gaussian and uniform disorder distribution with disorder parameter  $\Delta/U = 0.02$ . Image (c) correspond to an uniform disorder distribution with  $\Delta/U = 0.3$ .

Although the first-hopping order approximation for the effective action still leads to an equivalence between condensate and superfluid density, the result obtained with such method presents a more accurate behavior deep in the superfluid phase. Analogously to what we have shown in Chapter 3, even in the disordered case the mean-field prediction smoothly decreases as the hopping parameter increases, thus exhibiting a non-physical behavior. In contrast, the effective-action approach shows the density increasing linearly with the hopping parameter,

which is in agreement with the notion of a superfluid [26]. Therefore, the ever increasing condensate/superfluid density obtained with our field-theoretic method implies a larger range of validity of our theory. In the weak disorder regime,  $\Delta/U = 0.02$ , shown in images (a) and (b), respectively, both Gaussian and uniform disorder distributions present similar results. As the disorder parameter increases, the linear coefficient of the result for the effective-action method diminishes and the superfluid density increases more slowly, while the mean-field result decays rapidly (image (c)). Even though the analysis is made for weak disorder, the result of the effective-action approach already qualifies an improvement for the theory.

## 5.5 The Bose-glass phase

After the initial studies made by Fisher *et al.* [26] in 1989, intense research about the behavior of interacting bosons subject to static disorder took place. In order to investigate such behavior, one has to account for the competition between localizing effects caused by disorder and the delocalizing effects due to interactions which tend to excite particles out of their normally localized single-particle states. One important question raised in the above cited paper concerns whether a direct transition from a gaped Mott-insulating phase to a superfluid phase is possible in the presence of disorder. There, it was argued that such transition is unlikely to occur, suggesting the existence of a third phase between the other two: the Bose-glass phase. Over the years, different conclusions were reached about this issue [33, 34], however, the existence of the Bose glass was consistently proved [81–83].

A final conclusion was presented by L. Pollet *et al.* [84] in 2009 with the use of the so-called *theorem of inclusions*. Such theorem states that, in the presence of generic disorder, any transition presents rare but arbitrarily large regions of competing phases on either side of the phase boundary, provided the position of such boundary depends on the disorder distribution function. Generic disorder is defined as an arbitrary non-vanishing probability distribution of the disorder field within some bound. These large regions correspond to superfluid domains where the chemical potential is homogeneously shifted by  $\pm\Delta$ . No energy gap exists for particle transfer between such domains [85]. Therefore, no gaped Mott insulator can exist and the transition to the superfluid phase can only occur from the Bose-glass phase. Such argument is valid for arbitrarily weak disorder. The Bose glass is then characterized by either as localized single-particle levels or isolated superfluid lakes depending on the parameters of the system. Since the Bose glass does not allow phase coherence to spread through all the system's volume, it is identified by a finite density of states, finite compressibility, and gapless particle-hole excitations [77].

Although some characteristics of the Bose glass are well understood, detailed information about such phase are still lacking both from experimental and theoretical point of view. Here, we propose a new configuration of order parameters which could be used to identify each

phase of the disordered Bose-Hubbard model. In order to determine the superfluid phase we can define the condensate density  $n_0$  with use of the quantum and disorder ensemble averages of the bosonic creation and annihilation operators, i.e.,

$$\begin{aligned}\overline{\langle \hat{a}_i(\tau) \rangle} &= \psi \quad , \quad \overline{\langle \hat{a}_i^\dagger(\tau) \rangle} = \psi^* , \\ \psi^* \psi &= n_0.\end{aligned}\tag{5.29}$$

If we now calculate the variance  $q$  of such operators we get

$$\begin{aligned}q &= \overline{\langle (\hat{a}_i^\dagger(\tau) - \psi^*)(\hat{a}_i(\tau) - \psi) \rangle} \\ &= \overline{\langle \hat{a}_i^\dagger(\tau) \hat{a}_i(\tau) - \psi^* \hat{a}_i(\tau) - \hat{a}_i^\dagger(\tau) \psi + \psi^* \psi \rangle} \\ &= \overline{\langle \hat{a}_i^\dagger(\tau) \hat{a}_i(\tau) \rangle} - \psi^* \overline{\langle \hat{a}_i(\tau) \rangle} - \overline{\langle \hat{a}_i^\dagger(\tau) \rangle} \psi + \psi^* \psi,\end{aligned}\tag{5.30}$$

with the use of definitions (5.29) we can write

$$q + n_0 = \overline{\langle \hat{a}_i^\dagger(\tau) \hat{a}_i(\tau) \rangle},\tag{5.31}$$

where  $q$  is defined as a new order parameter to identify the Bose-glass phase. With the use of such order parameters the three phases can be characterized by the following:

- If  $n_0 \neq 0$  and  $q = 0$  we have the superfluid phase;
- If  $n_0 = 0$  and  $q \neq 0$  we have the Bose-glass phase;
- If both  $n_0 = q = 0$  we have the Mott-insulator phase.

The definition of such new order parameters is constructed similarly to Ref. [86]. In such paper the order parameter  $q$  is constructed in analogy with the Edwards-Anderson order parameter of the spin glasses theory [87], and it is argued that the introduction of such separate order parameter for the Bose glass is essential. Since disconnected condensate domains can form at sufficiently low temperatures, the system cannot be completely described by the usual BEC order parameter and is captured by Edwards-Anderson like order parameter.

With the use of the new order parameters introduced here, the theory discussed in this work could be reconstructed. The generating functionals necessary for the effective-action approach could be encountered by using expansions in such order parameters. By means of such order parameters, the analysis of the phase transition between superfluid and insulating phases in the disordered case may lead to more accurate results for the phase boundary. Also, detailed information about the Bose-glass phase may be found.

## 6 Summary and conclusion

The question of how the presence of disorder affects transport properties of quantum systems is an old problem which still engages many research. Some of the first studies of such question were made within the investigation of the superfluid properties of  $^4\text{He}$  in random media [88, 89]. As we have seen here, this problem was latter addressed in the context of bosonic ultracold systems subjected to random potentials [26]. As bosonic systems can form a BEC, with a macroscopic number of particles occupying the same quantum state, the combined effect of interactions and disorder drives the competition between superfluid and localized ground states. Recently, the advent of ultracold atomic states in optical lattices have provided extremely controllable environments to investigate the fundamental aspects of such phenomena.

In this work, we have shown how the Bose-Hubbard model, which describes bosonic particles hopping through an optical lattice, can be used to study such dirty boson problem with the introduction of diagonal disorder by means of a local chemical potential randomly distributed. We first presented how the bosonic system can be modeled with the BHH. As such Hamiltonian allows for the system to present different phases depending on the competition of its parameters, we used the theory of quantum phase transitions and presented the mean-field phase boundary and condensate density predictions. Some of the limitations of such theory were discussed. Considering the lack of precise analytical results in the literature, we constructed the general theory of the effective-action approach and proposed its application for dealing with the disordered Bose-Hubbard model. Such method makes use of field-theoretical considerations for the introduction of a source term into the BHH. With the use of perturbative methods, the generating functionals of the theory were calculated as an expansion in the sources as well as in the hopping parameter. By means of a Legendre transformation of the free-energy functional the effective action was found. Along with the introduction of a random chemical potential, it became necessary to consider a disorder ensemble average, which was used to define a new homogeneous order parameter for the static case. With the use of the Landau theory we studied the phase boundary between superfluid, Mott-insulator, and Bose-glass phases.

By using only the first-hopping order approximation for the effective-action method, we were able to reproduce the phase boundary prediction of the mean-field theory for the pure case as well as the results of Ref. [38] for homogeneous disorder distribution. This last result made it possible to observe the emergence of the Bose-glass phase between the Mott-insulating lobes as a consequence of finite temperature. For sufficient strong disorder, we could see that the Mott-insulator phase is destroyed and only superfluid and Bose-glass phase can exist. The finite temperature phase boundary for Gaussian disorder distribution was also obtained. As

such distribution extends to infinity, no Mott phase is allowed to exist and the only state below the critical line is the Bose glass. Furthermore, we compared the mean-field and effective-action predictions for the condensate/superfluid density in the disordered case. While the mean field prediction exhibits non-physical behavior, the result of our effective-action method turned out to present a consistently linearly increasing superfluid density as a function of the hopping parameter, which is in agreement with the theory of superfluidity.

The evidence of such results achieved within the framework of the effective-action approach applied to dirty bosons in optical lattices, opens up some new possibilities of investigations in the matter. In Section 5.5 we presented the definition of new order parameters, which could be used to reconstruct our theory and improve analytical results for the different phases of the system. By analyzing the poles of the correlation function, one can also study the spectrum of excitations. Lastly, as we have only considered the static case, dynamic properties may be explored further.

Finally, we conclude that our application of the effective-action approach to the studies of bosonic systems with disorder has been successful. The method showed to be promising by presenting an agreement with former analytical results and even an improvement of such results for the calculation of some quantities, such as the condensate density, deep in the superfluid phase. We expect our analysis to be the starting point for future investigations and applications of the effective-action approach when dealing with disordered systems.

# Bibliography

- [1] S. N. Bose, "Plancks gesetz und lichtquantenhypothese," *Z. Physik*, 1924.
- [2] A. Einstein, "Quantentheorie des einatomigen idealen gases. akademie der wissenschaften," *Kommission bei W. de Gruyter*, p. 2, 1924.
- [3] A. Einstein, "Quantentheorie des einatomigen idealen gases. zweite ab- handlung, sitzungsberichte der preußischen akademie der wissenschaf ten (berlin).," *Physikalisch-mathematische Klasse*, pp. 3–14, 1925.
- [4] F. London, "The  $\lambda$ -phenomenon of liquid helium and the bose-einstein degeneracy," *Nature*, vol. 141, no. 3571, p. 643, 1938.
- [5] E. Svensson and V. Sears, "Neutron scattering by 4he and 3he," *Physica B+ C*, vol. 137, no. 1-3, pp. 126–140, 1986.
- [6] W. D. Phillips, "Nobel lecture: Laser cooling and trapping of neutral atoms," *Reviews of Modern Physics*, vol. 70, no. 3, p. 721, 1998.
- [7] S. Chu, "Nobel lecture: The manipulation of neutral particles," *Reviews of Modern Physics*, vol. 70, no. 3, p. 685, 1998.
- [8] C. N. Cohen-Tannoudji, "Nobel lecture: Manipulating atoms with photons," *Reviews of Modern Physics*, vol. 70, no. 3, p. 707, 1998.
- [9] "The nobel prize in physics 1997 - nobelprize.org." <https://www.nobelprize.org/prizes/physics/1997/summary/>. Accessed: 2019-01-07.
- [10] M. H. Anderson, J. R. Ensher, M. R. Matthews, C. E. Wieman, and E. A. Cornell, "Observation of bose-einstein condensation in a dilute atomic vapor," *Science*, vol. 269, no. 5221, pp. 198–201, 1995.
- [11] K. B. Davis, M.-O. Mewes, M. R. Andrews, N. Van Druten, D. Durfee, D. Kurn, and W. Ketterle, "Bose-einstein condensation in a gas of sodium atoms," *Physical review letters*, vol. 75, no. 22, p. 3969, 1995.
- [12] C. C. Bradley, C. Sackett, J. Tollett, and R. G. Hulet, "Evidence of bose-einstein condensation in an atomic gas with attractive interactions," *Physical Review Letters*, vol. 75, no. 9, p. 1687, 1995.
- [13] "The nobel prize in physics 2001 - nobelprize.org." <https://www.nobelprize.org/prizes/physics/2001/press-release/>. Accessed: 2019-01-07.



- [14] "Bose-Einstein Condensate graph." <https://www.jpl.nasa.gov/spaceimages/details.php?id=PIA22561>. Accessed: 2018-11-21.
- [15] A. Griffin, D. W. Snoke, and S. Stringari, *Bose-einstein condensation*. Cambridge University Press, 1996.
- [16] I. Bloch, "Ultracold quantum gases in optical lattices," *Nature Physics*, vol. 1, no. 1, p. 23, 2005.
- [17] H. Moritz, T. Stöferle, M. Köhl, and T. Esslinger, "Exciting collective oscillations in a trapped 1d gas," *Physical review letters*, vol. 91, no. 25, p. 250402, 2003.
- [18] T. Stöferle, H. Moritz, C. Schori, M. Köhl, and T. Esslinger, "Transition from a strongly interacting 1d superfluid to a mott insulator," *Physical review letters*, vol. 92, no. 13, p. 130403, 2004.
- [19] A. Hemmerich and T. Hänsch, "Two-dimensional atomic crystal bound by light," *Physical review letters*, vol. 70, no. 4, p. 410, 1993.
- [20] G. Grynberg, B. Lounis, P. Verkerk, J.-Y. Courtois, and C. Salomon, "Quantized motion of cold cesium atoms in two-and three-dimensional optical potentials," *Physical review letters*, vol. 70, no. 15, p. 2249, 1993.
- [21] C. Becker, P. Soltan-Panahi, J. Kronjäger, S. Dörscher, K. Bongs, and K. Sengstock, "Ultracold quantum gases in triangular optical lattices," *New Journal of Physics*, vol. 12, no. 6, p. 065025, 2010.
- [22] G.-B. Jo, J. Guzman, C. K. Thomas, P. Hosur, A. Vishwanath, and D. M. Stamper-Kurn, "Ultracold atoms in a tunable optical kagome lattice," *Physical review letters*, vol. 108, no. 4, p. 045305, 2012.
- [23] M. Greiner, *Ultracold quantum gases in three-dimensional optical lattice potentials*. PhD thesis, Imu, 2003.
- [24] O. Morsch and M. Oberthaler, "Dynamics of bose-einstein condensates in optical lattices," *Reviews of modern physics*, vol. 78, no. 1, p. 179, 2006.
- [25] D. Jaksch, C. Bruder, J. I. Cirac, C. W. Gardiner, and P. Zoller, "Cold bosonic atoms in optical lattices," *Physical Review Letters*, vol. 81, no. 15, p. 3108, 1998.
- [26] M. P. Fisher, P. B. Weichman, G. Grinstein, and D. S. Fisher, "Boson localization and the superfluid-insulator transition," *Physical Review B*, vol. 40, no. 1, p. 546, 1989.
- [27] M. Greiner, O. Mandel, T. Esslinger, T. W. Hänsch, and I. Bloch, "Quantum phase transition from a superfluid to a mott insulator in a gas of ultracold atoms," *Nature*, vol. 415, no. 6867, p. 39, 2002.

- [28] T. Khellil and A. Pelster, "Hartree–fock mean-field theory for trapped dirty bosons," *Journal of Statistical Mechanics: Theory and Experiment*, vol. 2016, no. 6, p. 063301, 2016.
- [29] T. Khellil, A. Balaž, and A. Pelster, "Analytical and numerical study of dirty bosons in a quasi-one-dimensional harmonic trap," *New Journal of Physics*, vol. 18, no. 6, p. 063003, 2016.
- [30] T. Khellil and A. Pelster, "Dirty bosons in a three-dimensional harmonic trap," *Journal of Statistical Mechanics: Theory and Experiment*, vol. 2017, no. 9, p. 093108, 2017.
- [31] J. Lye, L. Fallani, M. Modugno, D. Wiersma, C. Fort, and M. Inguscio, "Bose-einstein condensate in a random potential," *Physical review letters*, vol. 95, no. 7, p. 070401, 2005.
- [32] D. Clément, A. F. Varon, M. Hugbart, J. A. Retter, P. Bouyer, L. Sanchez-Palencia, D. M. Gangardt, G. V. Shlyapnikov, and A. Aspect, "Suppression of transport of an interacting elongated bose-einstein condensate in a random potential," *Physical Review Letters*, vol. 95, no. 17, p. 170409, 2005.
- [33] W. Krauth, N. Trivedi, and D. Ceperley, "Superfluid-insulator transition in disordered boson systems," *Physical review letters*, vol. 67, no. 17, p. 2307, 1991.
- [34] J. Kisker and H. Rieger, "Bose-glass and mott-insulator phase in the disordered boson hubbard model," *Physical Review B*, vol. 55, no. 18, p. R11981, 1997.
- [35] J. Freericks and H. Monien, "Strong-coupling expansions for the pure and disordered bose-hubbard model," *Physical Review B*, vol. 53, no. 5, p. 2691, 1996.
- [36] R. T. Scalettar, G. G. Batrouni, and G. T. Zimanyi, "Localization in interacting, disordered, bose systems," *Physical review letters*, vol. 66, no. 24, p. 3144, 1991.
- [37] P. B. Weichman, "Dirty bosons: Twenty years later," *Modern Physics Letters B*, vol. 22, no. 27, pp. 2623–2647, 2008.
- [38] K. Krutitsky, A. Pelster, and R. Graham, "Mean-field phase diagram of disordered bosons in a lattice at nonzero temperature," *New Journal of Physics*, vol. 8, no. 9, p. 187, 2006.
- [39] B. Capogrosso-Sansone, N. Prokof'Ev, and B. Svistunov, "Phase diagram and thermodynamics of the three-dimensional bose-hubbard model," *Physical Review B*, vol. 75, no. 13, p. 134302, 2007.
- [40] F. Dos Santos and A. Pelster, "Quantum phase diagram of bosons in optical lattices," *Physical Review A*, vol. 79, no. 1, p. 013614, 2009.

- [41] B. Bradlyn, F. E. A. Dos Santos, and A. Pelster, "Effective action approach for quantum phase transitions in bosonic lattices," *Physical Review A*, vol. 79, no. 1, p. 013615, 2009.
- [42] F. E. A. dos Santos, *Ginzburg-Landau theory for bosonic gases in optical lattices*. PhD thesis, Freie Universität Berlin, 2011.
- [43] Y.-W. Lee and M.-F. Yang, "Superfluid-insulator transitions in attractive bose-hubbard model with three-body constraint," *Physical Review A*, vol. 81, no. 6, p. 061604, 2010.
- [44] X.-F. Zhou, Y.-S. Zhang, and G.-C. Guo, "Pair tunneling of bosonic atoms in an optical lattice," *Physical Review A*, vol. 80, no. 1, p. 013605, 2009.
- [45] O. Mandel, M. Greiner, A. Widera, T. Rom, T. W. Hänsch, and I. Bloch, "Controlled collisions for multi-particle entanglement of optically trapped atoms," *Nature*, vol. 425, no. 6961, p. 937, 2003.
- [46] Ş. G. Söyler, B. Capogrosso-Sansone, N. Prokof'ev, and B. Svistunov, "Sign-alternating interaction mediated by strongly correlated lattice bosons," *New Journal of Physics*, vol. 11, no. 7, p. 073036, 2009.
- [47] N. Teichmann, D. Hinrichs, and M. Holthaus, "Reference data for phase diagrams of triangular and hexagonal bosonic lattices," *EPL (Europhysics Letters)*, vol. 91, no. 1, p. 10004, 2010.
- [48] L. Santos, M. Baranov, J. I. Cirac, H.-U. Everts, H. Fehrmann, and M. Lewenstein, "Atomic quantum gases in kagomé lattices," *Physical review letters*, vol. 93, no. 3, p. 030601, 2004.
- [49] B. H. Bransden and C. J. Joachain, *Physics of atoms and molecules*. Longman Scientific and Technical, 1983.
- [50] R. Grimm, M. Weidemüller, and Y. B. Ovchinnikov, "Optical dipole traps for neutral atoms," in *Advances in atomic, molecular, and optical physics*, vol. 42, pp. 95–170, Elsevier, 2000.
- [51] C. J. Foot *et al.*, *Atomic physics*, vol. 7. Oxford University Press, 2005.
- [52] C. J. Pethick and H. Smith, *Bose-Einstein condensation in dilute gases*. Cambridge university press, 2002.
- [53] D. Meschede, *Optics, light and lasers: the practical approach to modern aspects of photonics and laser physics*. John Wiley & Sons, 2017.
- [54] H. J. Metcalf and P. Van der Straten, *Laser cooling and trapping*. Springer Science & Business Media, 2012.

- [55] L. Pitaevskii and S. Stringari, *Bose-Einstein condensation and superfluidity*, vol. 164. Oxford University Press, 2016.
- [56] A. J. Leggett, *Quantum liquids: Bose condensation and Cooper pairing in condensed-matter systems*. Oxford University Press, 2006.
- [57] A. L. Fetter and J. D. Walecka, *Quantum theory of many-particle systems*. Courier Corporation, 2012.
- [58] K. V. Krutitsky, "Ultracold bosons with short-range interaction in regular optical lattices," *Physics Reports*, vol. 607, pp. 1–101, 2016.
- [59] D. Jaksch and P. Zoller, "The cold atom hubbard toolbox," *Annals of physics*, vol. 315, no. 1, pp. 52–79, 2005.
- [60] A. Albus, F. Illuminati, and J. Eisert, "Mixtures of bosonic and fermionic atoms in optical lattices," *Physical Review A*, vol. 68, no. 2, p. 023606, 2003.
- [61] R. Pathria, "Statistical mechanics, international series in natural philosophy," 1986.
- [62] K. Huang, "Statistical mechanics," 1987.
- [63] S. Sachdev, *Quantum phase transitions*. Cambridge university press, 2011.
- [64] L. D. Landau, "On the theory of phase transitions," *Ukr. J. Phys.*, vol. 11, pp. 19–32, 1937.
- [65] J. Y. Fu, "On the landau theory of phase transitions: a hierarchical dynamic model," *Journal of Physics: Condensed Matter*, vol. 25, no. 7, p. 075903, 2013.
- [66] N. Teichmann and D. Hinrichs, "Scaling property of the critical hopping parameters for the bose-hubbard model," *The European Physical Journal B*, vol. 71, no. 2, p. 219, 2009.
- [67] R. Roth and K. Burnett, "Superfluidity and interference pattern of ultracold bosons in optical lattices," *Physical Review A*, vol. 67, no. 3, p. 031602, 2003.
- [68] M. Kübler, F. Sant'Ana, F. dos Santos, and A. Pelster, "Improving mean-field theory for bosons in optical lattices via degenerate perturbation theory," *arXiv preprint arXiv:1804.08689*, 2018.
- [69] J. Zinn-Justin, *Quantum field theory and critical phenomena*. Clarendon Press, 1996.
- [70] H. Kleinert and V. Schulte-Frohlinde, *Critical Properties of  $\phi^4$ -theories*. World Scientific, 2001.
- [71] M. Ohliger and A. Pelster, "Green's function approach to the bose-hubbard model," *arXiv preprint arXiv:0810.4399*, 2008.

- [72] W. Metzner, "Linked-cluster expansion around the atomic limit of the hubbard model," *Physical Review B*, vol. 43, no. 10, p. 8549, 1991.
- [73] M. P. Gelfand, R. R. Singh, and D. A. Huse, "Perturbation expansions for quantum many-body systems," *Journal of Statistical Physics*, vol. 59, no. 5-6, pp. 1093–1142, 1990.
- [74] A. Irving and C. Hamer, "Methods in hamiltonian lattice field theory (ii). linked-cluster expansions," *Nuclear Physics B*, vol. 230, no. 3, pp. 361–384, 1984.
- [75] H. Kleinert, *Path integrals in quantum mechanics, statistics, polymer physics, and financial markets*. World scientific, 2009.
- [76] T. Matsubara, "A new approach to quantum-statistical mechanics," *Progress of theoretical physics*, vol. 14, no. 4, pp. 351–378, 1955.
- [77] V. Gurarie, L. Pollet, N. Prokof'Ev, B. Svistunov, and M. Troyer, "Phase diagram of the disordered bose-hubbard model," *Physical Review B*, vol. 80, no. 21, p. 214519, 2009.
- [78] U. Bissbort, R. Thomale, and W. Hofstetter, "Stochastic mean-field theory: Method and application to the disordered bose-hubbard model at finite temperature and speckle disorder," *Physical Review A*, vol. 81, no. 6, p. 063643, 2010.
- [79] D. Van Oosten, P. van der Straten, and H. Stoof, "Quantum phases in an optical lattice," *Physical Review A*, vol. 63, no. 5, p. 053601, 2001.
- [80] D. Dickerscheid, D. Van Oosten, P. Denteneer, and H. Stoof, "Ultracold atoms in optical lattices," *Physical Review A*, vol. 68, no. 4, p. 043623, 2003.
- [81] B. Damski, J. Zakrzewski, L. Santos, P. Zoller, and M. Lewenstein, "Atomic bose and anderson glasses in optical lattices," *Physical review letters*, vol. 91, no. 8, p. 080403, 2003.
- [82] L. Fallani, J. Lye, V. Guarrera, C. Fort, and M. Inguscio, "Ultracold atoms in a disordered crystal of light: Towards a bose glass," *Physical review letters*, vol. 98, no. 13, p. 130404, 2007.
- [83] I. F. Herbut, "Dual theory of the superfluid-bose-glass transition in the disordered bose-hubbard model in one and two dimensions," *Physical Review B*, vol. 57, no. 21, p. 13729, 1998.
- [84] L. Pollet, N. Prokof'ev, B. Svistunov, and M. Troyer, "Absence of a direct superfluid to mott insulator transition in disordered bose systems," *Physical review letters*, vol. 103, no. 14, p. 140402, 2009.

- [85] P. B. Weichman and R. Mukhopadhyay, "Particle-hole symmetry and the dirty boson problem," *Physical Review B*, vol. 77, no. 21, p. 214516, 2008.
- [86] R. Graham and A. Pelster, "Order via nonlinearity in randomly confined bose gases," *International Journal of Bifurcation and Chaos*, vol. 19, no. 08, pp. 2745–2753, 2009.
- [87] S. F. Edwards and P. W. Anderson, "Theory of spin glasses," *Journal of Physics F: Metal Physics*, vol. 5, no. 5, p. 965, 1975.
- [88] S. A. Khairallah and D. Ceperley, "Superfluidity of dense he 4 in vycor," *Physical review letters*, vol. 95, no. 18, p. 185301, 2005.
- [89] M. Chan, A. Yanof, and J. Reppy, "Superfluidity of thin he 4 films," *Physical Review Letters*, vol. 32, no. 24, p. 1347, 1974.

# A Appendix 1

In this appendix we calculate the expression use in Chapter 4 for the four-point Green's function  $G_{0i}^{(4)}$  in Matsubara space. We can start by considering a general multiple integral of the form

$$G(\omega_n, \dots, \omega_1) = \int_0^\beta d\tau_n \cdots \int_0^\beta d\tau_1 e^{i(\omega_1\tau_1 + \dots + \omega_n\tau_n)} \text{Tr} \left\{ e^{-\beta\hat{H}} \hat{T} [\hat{O}_n(\tau_n) \dots \hat{O}_1(\tau_1)] \right\}, \quad (\text{A.1})$$

where  $\omega_n = (2\pi/\beta)n$  are the Matsubara frequencies with  $n$  integer,  $\hat{H}$  is an arbitrary time-independent Hamiltonian, and  $\hat{O}_n(\tau_n)$  are arbitrary operators in the Heisenberg picture, i.e.,  $\hat{O}_i(\tau_i) = e^{\tau_i\hat{H}} \hat{O}_i(0) e^{-\tau_i\hat{H}}$ . The invariance of the trace under cyclic permutations makes it possible to write

$$\text{Tr} \left\{ e^{-\beta\hat{H}} \hat{T} [\hat{O}_n(\tau_n) \dots \hat{O}_1(\tau_1)] \right\} = \text{Tr} \left\{ e^{-\beta\hat{H}} \hat{T} [\hat{O}_n(\tau_n - \tau_1) \dots \hat{O}_2(\tau_2 - \tau_1) \hat{O}_1(0)] \right\}. \quad (\text{A.2})$$

If we use the transformation  $\tau_i \rightarrow \tau_i + \tau_1$  in the imaginary-time variables  $\{\tau_n, \dots, \tau_2\}$  equation (A.1) becomes

$$\begin{aligned} G(\omega_n, \dots, \omega_1) &= \int_0^\beta d\tau_1 e^{i(\omega_1 + \dots + \omega_n)\tau_1} \\ &\times \int_{-\tau_1}^{\beta-\tau_1} d\tau_n \cdots \int_{-\tau_1}^{\beta-\tau_1} d\tau_2 e^{i(\omega_2\tau_2 + \dots + \omega_n\tau_n)} \text{Tr} \left\{ e^{-\beta\hat{H}} \hat{T} [\hat{O}_n(\tau_n) \dots \hat{O}_2(\tau_2) \hat{O}_1(0)] \right\}. \end{aligned} \quad (\text{A.3})$$

By splitting the interval of integration the tow semi intervals  $[-\tau_1, 0]$  and  $[0, \beta - \tau_1]$  we can write

$$\begin{aligned} &\int_{-\tau_1}^{\beta-\tau_1} d\tau_n \cdots \int_{-\tau_1}^{\beta-\tau_1} d\tau_2 e^{i(\omega_2\tau_2 + \dots + \omega_n\tau_n)} \text{Tr} \left\{ e^{-\beta\hat{H}} \hat{T} [\hat{O}_n(\tau_n) \dots \hat{O}_2(\tau_2) \hat{O}_1(0)] \right\} \\ &= \left( \int_{-\tau_1}^0 d\tau_n + \int_0^{\beta-\tau_1} d\tau_n \right) \cdots \left( \int_{-\tau_1}^0 d\tau_2 + \int_0^{\beta-\tau_1} d\tau_2 \right) e^{i(\omega_2\tau_2 + \dots + \omega_n\tau_n)} \\ &\times \text{Tr} \left\{ e^{-\beta\hat{H}} \hat{T} [\hat{O}_n(\tau_n) \dots \hat{O}_2(\tau_2) \hat{O}_1(0)] \right\}. \end{aligned} \quad (\text{A.4})$$

Such expression is composed by a sum of multiple integrals in each semi interval. If we consider an arbitrary term which presents  $l - 1$  imaginary-time variables  $\{\tau_{i_l}, \dots, \tau_{i_2}\}$  integrated over the interval  $[0, \beta - \tau_1]$  and  $n - l$  imaginary-time variables  $\{\tau_{i_n}, \dots, \tau_{i_{l+1}}\}$  integrated over the interval  $[-\tau_1, 0]$ , i.e.,

$$\begin{aligned} &\int_{-\tau_1}^0 d\tau_{i_n} \cdots \int_{-\tau_1}^0 d\tau_{i_{l+1}} \int_0^{\beta-\tau_1} d\tau_{i_l} \cdots \int_0^{\beta-\tau_1} d\tau_{i_2} \\ &\times e^{i(\omega_{i_2}\tau_{i_2} + \dots + \omega_{i_n}\tau_{i_n})} \text{Tr} \left\{ e^{-\beta\hat{H}} \hat{T} [\hat{O}_{i_n}(\tau_{i_n}) \dots \hat{O}_{i_2}(\tau_{i_2}) \hat{O}_1(0)] \right\} \\ &= \int_{-\tau_1}^0 d\tau_{i_n} \cdots \int_{-\tau_1}^0 d\tau_{i_{l+1}} \int_0^{\beta-\tau_1} d\tau_{i_l} \cdots \int_0^{\beta-\tau_1} d\tau_{i_2} \\ &\times e^{i(\omega_{i_2}\tau_{i_2} + \dots + \omega_{i_n}\tau_{i_n})} \text{Tr} \left\{ e^{-\beta\hat{H}} \hat{T} [\hat{O}_{i_l}(\tau_{i_l}) \dots \hat{O}_{i_2}(\tau_{i_2})] \hat{O}_1(0) \hat{T} [\hat{O}_{i_n}(\tau_{i_n}) \dots \hat{O}_{i_{l+1}}(\tau_{i_{l+1}})] \right\}, \end{aligned} \quad (\text{A.5})$$

where we have observed that  $\tau < 0$  if  $\tau \in \{\tau_{i_n}, \dots, \tau_{i_{l+1}}\}$  and  $\tau > 0$  if  $\tau \in \{\tau_{i_l}, \dots, \tau_{i_2}\}$ .

We now make use of the transformation  $\tau \rightarrow \tau - \beta$ , in the variables  $\{\tau_{i_n}, \dots, \tau_{i_{l+1}}\}$  which gives

$$\begin{aligned}
& \int_{-\tau_1}^0 d\tau_{i_n} \cdots \int_{-\tau_1}^0 d\tau_{i_{l+1}} \int_0^{\beta-\tau_1} d\tau_{i_l} \cdots \int_0^{\beta-\tau_1} d\tau_{i_2} \\
& \quad \times e^{i(\omega_{i_2}\tau_{i_2} + \cdots + \omega_{i_n}\tau_{i_n})} \text{Tr} \left\{ e^{-\beta\hat{H}} \hat{T} \left[ \hat{O}_{i_n}(\tau_{i_n}) \cdots \hat{O}_{i_2}(\tau_{i_2}) \hat{O}_1(0) \right] \right\} \\
& = \int_{\beta-\tau_1}^{\beta} d\tau_{i_n} \cdots \int_{\beta-\tau_1}^{\beta} d\tau_{i_{l+1}} \int_0^{\beta-\tau_1} d\tau_{i_l} \cdots \int_0^{\beta-\tau_1} d\tau_{i_2} e^{i(\omega_{i_2}\tau_{i_2} + \cdots + \omega_{i_n}\tau_{i_n})} \\
& \quad \times \text{Tr} \left\{ e^{-\beta\hat{H}} \hat{T} \left[ \hat{O}_{i_l}(\tau_{i_l}) \cdots \hat{O}_{i_2}(\tau_{i_2}) \right] \hat{O}_1(0) e^{-\beta\hat{H}} \hat{T} \left[ \hat{O}_{i_n}(\tau_{i_n}) \cdots \hat{O}_{i_{l+1}}(\tau_{i_{l+1}}) \right] e^{\beta\hat{H}} \right\} \\
& = \int_{\beta-\tau_1}^{\beta} d\tau_{i_n} \cdots \int_{\beta-\tau_1}^{\beta} d\tau_{i_{l+1}} \int_0^{\beta-\tau_1} d\tau_{i_l} \cdots \int_0^{\beta-\tau_1} d\tau_{i_2} e^{i(\omega_{i_2}\tau_{i_2} + \cdots + \omega_{i_n}\tau_{i_n})} \\
& \quad \times \text{Tr} \left\{ e^{-\beta\hat{H}} \hat{T} \left[ \hat{O}_{i_n}(\tau_{i_n}) \cdots \hat{O}_{i_{l+1}}(\tau_{i_{l+1}}) \right] \hat{T} \left[ \hat{O}_{i_l}(\tau_{i_l}) \cdots \hat{O}_{i_2}(\tau_{i_2}) \right] \hat{O}_1(0) \right\} \\
& = \int_{\beta-\tau_1}^{\beta} d\tau_{i_n} \cdots \int_{\beta-\tau_1}^{\beta} d\tau_{i_{l+1}} \int_0^{\beta-\tau_1} d\tau_{i_l} \cdots \int_0^{\beta-\tau_1} d\tau_{i_2} e^{i(\omega_{i_2}\tau_{i_2} + \cdots + \omega_{i_n}\tau_{i_n})} \\
& \quad \times \text{Tr} \left\{ e^{-\beta\hat{H}} \hat{T} \left[ \hat{O}_{i_n}(\tau_{i_n}) \cdots \hat{O}_{i_2}(\tau_{i_2}) \hat{O}_1(0) \right] \right\}.
\end{aligned} \tag{A.6}$$

Thus, the limits of integration  $[-\tau_1, 0]$  in equation (A.4) can be substituted by  $[\beta - \tau_1, \beta]$  which gives

$$\begin{aligned}
& \left( \int_{-\tau_1}^0 d\tau_n + \int_0^{\beta-\tau_1} d\tau_n \right) \cdots \left( \int_{-\tau_1}^0 d\tau_2 + \int_0^{\beta-\tau_1} d\tau_2 \right) e^{i(\omega_2\tau_2 + \cdots + \omega_n\tau_n)} \\
& \quad \times \text{Tr} \left\{ e^{-\beta\hat{H}} \hat{T} \left[ \hat{O}_n(\tau_n) \cdots \hat{O}_2(\tau_2) \hat{O}_1(0) \right] \right\} \\
& = \left( \int_0^{\beta-\tau_1} d\tau_n + \int_{\beta-\tau_1}^{\beta} d\tau_n \right) \cdots \left( \int_0^{\beta-\tau_1} d\tau_2 + \int_{\beta-\tau_1}^{\beta} d\tau_2 \right) e^{i(\omega_2\tau_2 + \cdots + \omega_n\tau_n)} \\
& \quad \times \text{Tr} \left\{ e^{-\beta\hat{H}} \hat{T} \left[ \hat{O}_n(\tau_n) \cdots \hat{O}_2(\tau_2) \hat{O}_1(0) \right] \right\} \\
& = \int_0^{\beta} d\tau_n \cdots \int_0^{\beta} d\tau_2 e^{i(\omega_2\tau_2 + \cdots + \omega_n\tau_n)} \text{Tr} \left\{ e^{-\beta\hat{H}} \hat{T} \left[ \hat{O}_n(\tau_n) \cdots \hat{O}_2(\tau_2) \hat{O}_1(0) \right] \right\}.
\end{aligned} \tag{A.7}$$

With this result, equation (A.3) can be written as

$$\begin{aligned}
G(\omega_n, \dots, \omega_1) & = \beta \delta_{0, \omega_n + \cdots + \omega_1} \int_0^{\beta} d\tau_n \cdots \int_0^{\beta} d\tau_2 \\
& \quad \times e^{i(\omega_2\tau_2 + \cdots + \omega_n\tau_n)} \text{Tr} \left\{ e^{-\beta\hat{H}} \hat{T} \left[ \hat{O}_n(\tau_n) \cdots \hat{O}_2(\tau_2) \hat{O}_1(0) \right] \right\}.
\end{aligned} \tag{A.8}$$

Therefore, we can write the four-point function  $G_{0i}^{(4)}$  in Matsubara space as

$$\begin{aligned}
G_{0i}^{(4)}(\omega_1, \omega_2; \omega'_1, \omega'_2) & = \beta \delta_{\omega'_1 + \omega'_2, \omega_1 + \omega_2} \\
& \quad \times \int_0^{\beta} d\tau_1 \int_0^{\beta} d\tau_2 \int_0^{\beta} d\tau'_1 e^{-i(\omega_1\tau_1 + \omega_2\tau_2 - \omega'_1\tau'_1)} G_{0i}^{(4)}(\tau_1, \tau_2; \tau'_1, 0).
\end{aligned} \tag{A.9}$$



Using the expression of equation (4.71) we get

$$\begin{aligned}
G_{0i}^{(4)}(\omega_1, \omega_2; \omega'_1, \omega'_2) &= \frac{\beta}{Z_{0i}^{(0)}} \delta_{\omega'_1 + \omega'_2, \omega_1 + \omega_2} \\
&\times \sum_{n=0}^{\infty} e^{-\beta f_i(n)} \\
&\times \{(n+1)^2 \\
&\quad \times I[i\omega_2 + f_i(n) - f_i(n+1), -i\omega'_1 + f_i(n+1) - f_i(n), i\omega_1 + f_i(n) - f_i(n+1)] \\
&\quad + (n+2)(n+1) \\
&\quad \times I[i\omega_2 + f_i(n) - f_i(n+1), i\omega_1 + f_i(n+1) - f_i(n+2), -i\omega'_1 + f_i(n+2) - f_i(n+1)] \\
&\quad + n(n+1) \\
&\quad \times I[-i\omega'_1 + f_i(n) - f_i(n-1), i\omega_2 + f_i(n-1) - f_i(n), i\omega_1 + f_i(n) - f_i(n+1)] \\
&\quad + \omega'_1 \leftrightarrow \omega_1\},
\end{aligned} \tag{A.10}$$

where we have defined

$$I[x_3, x_2, x_1] = \int_0^\beta d\tau_3 \int_0^{\tau_3} d\tau_2 \int_0^{\tau_2} d\tau_1 e^{x_3 \tau_3 + x_2 \tau_2 + x_1 \tau_1}. \tag{A.11}$$

Direct calculation of such integrals yields

$$\begin{aligned}
&I[i\omega_2 + f_i(n) - f_i(n+1), -i\omega'_1 + f_i(n+1) - f_i(n), i\omega_1 + f_i(n) - f_i(n+1)] \\
&= \frac{e^{-\beta[f_i(n+1) - f_i(n)]} - 1}{[i\omega_1 + f_i(n+1) - f_i(n+2)][i\omega_2 + f_i(n) - f_i(n+1)][-i\omega'_1 + f_i(n+2) - f_i(n+1)]} \\
&\quad - \frac{e^{-\beta[f_i(n+2) - f_i(n)]} - 1}{[i\omega_1 + f_i(n+1) - f_i(n+2)][i\omega_1 + i\omega_2 + f_i(n) - f_i(n+2)][-i\omega'_1 + f_i(n+2) - f_i(n+1)]} \\
&+ \frac{\beta \delta_{\omega_1, \omega'_1} e^{-\beta[f_i(n+1) - f_i(n)]}}{[-i\omega'_1 + f_i(n+2) - f_i(n+1)][i\omega_2 + f_i(n) - f_i(n+1)]} \\
&\quad - \frac{e^{-\beta[f_i(n+1) - f_i(n)]} - 1}{[-i\omega'_1 + f_i(n+2) - f_i(n+1)][i\omega_1 + i\omega_2 - i\omega'_1 + f_i(n) - f_i(n+1)][i\omega_2 + f_i(n) - f_i(n+1)]},
\end{aligned} \tag{A.12}$$

$$\begin{aligned}
&I[-i\omega'_1 + f_i(n) - f_i(n-1), i\omega_2 + f_i(n-1) - f_i(n), i\omega_1 + f_i(n) - f_i(n+1)] \\
&= \frac{e^{-\beta[f_i(n-1) - f_i(n)]} - 1}{[i\omega_1 + f_i(n) - f_i(n+1)][i\omega_2 + f_i(n-1) - f_i(n)][-i\omega'_1 + f_i(n) - f_i(n-1)]} \\
&\quad - \frac{e^{-\beta[f_i(n-1) - f_i(n)]} - 1}{[i\omega_1 + f_i(n) - f_i(n+1)][i\omega_1 + i\omega_2 + f_i(n-1) - f_i(n+1)][-i\omega'_1 + f_i(n) - f_i(n-1)]} \\
&\quad - \frac{\beta \delta_{\omega_2, \omega'_1}}{[i\omega_1 + f_i(n) - f_i(n+1)][i\omega_2 + f_i(n-1) - f_i(n)]} \\
&\quad - \frac{e^{-\beta[f_i(n+1) - f_i(n)]} - 1}{[i\omega_1 + f_i(n) - f_i(n+1)][i\omega_1 + i\omega_2 - i\omega'_1 + f_i(n) - f_i(n+1)][i\omega_1 + i\omega_2 + f_i(n-1) - f_i(n+2)]},
\end{aligned} \tag{A.13}$$

$$\begin{aligned}
& I[i\omega_2 + f_i(n) - f_i(n+1), i\omega_1 + f_i(n+1) - f_i(n+2), -i\omega'_1 + f_i(n+2) - f_i(n+1)] \\
&= \frac{e^{-\beta[f_i(n+1)-f_i(n)]} - 1}{[i\omega_1 + f_i(n) - f_i(n+1)][i\omega_2 + f_i(n) - f_i(n+1)][-i\omega'_1 + f_i(n+1) - f_i(n)]} \\
&- \frac{\beta\delta_{\omega_2, \omega'_1}}{[i\omega_1 + f_i(n) - f_i(n+1)][i\omega_2 + f_i(n-1) - f_i(n)]} \\
&+ \frac{\beta\delta_{\omega_2, \omega'_1} e^{-\beta[f_i(n+1)-f_i(n)]}}{[-i\omega'_1 + f_i(n) - f_i(n+1)][i\omega_2 + f_i(n) - f_i(n+1)]} \\
&- \frac{e^{-\beta[f_i(n+1)-f_i(n)]} - 1}{[i\omega_1 + f_i(n) - f_i(n+1)][i\omega_1 + i\omega_2 - i\omega'_1 + f_i(n) - f_i(n+1)][i\omega_2 + f_i(n) - f_i(n+1)]}. \tag{A.14}
\end{aligned}$$

By substituting these results in equation (A.10) and applying the condition  $\omega'_1 + \omega'_2 = \omega_1 + \omega_2$  we can obtain equation (4.72).